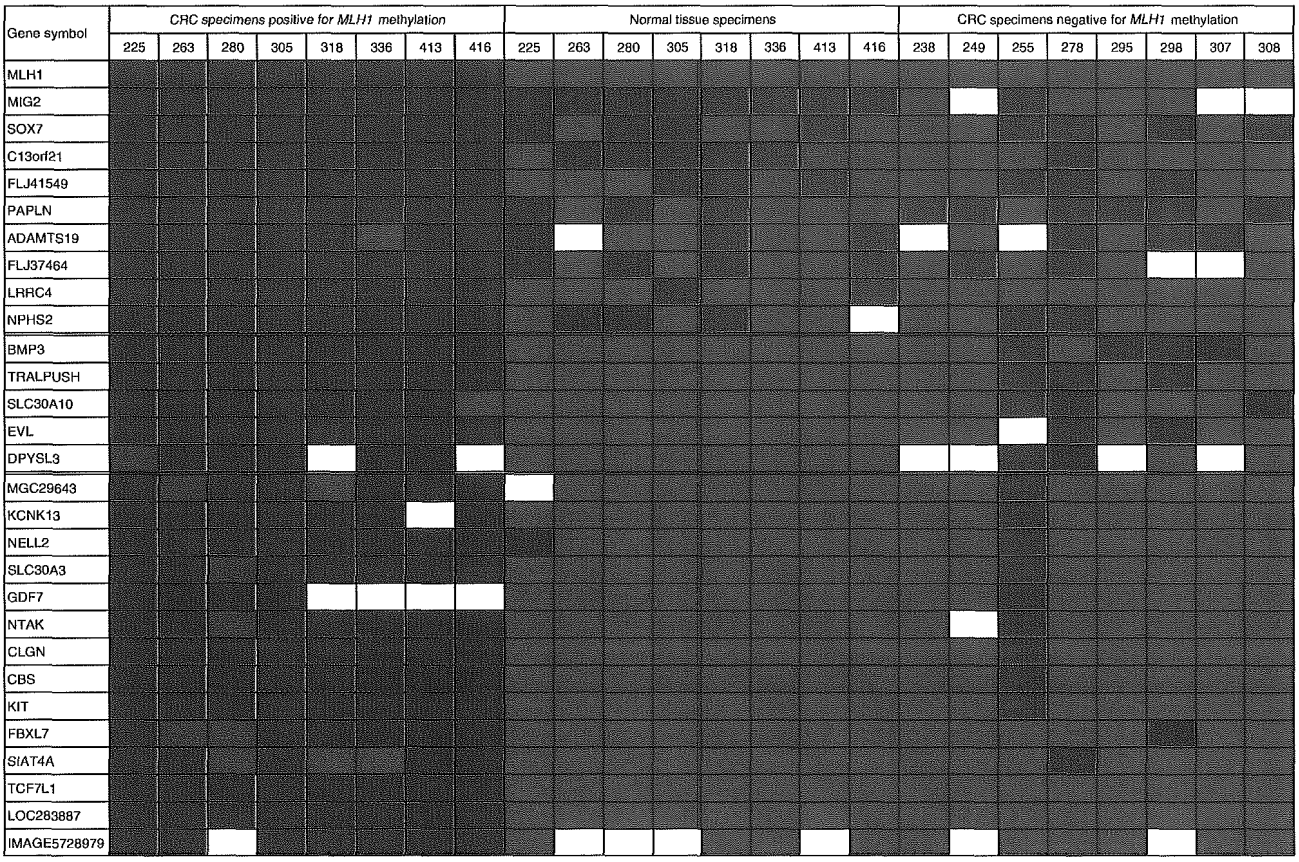

Fig. 1. Gene methylation profiles of CRC specimens. Twenty-eight clones were randomly chosen from the MCA–RDA products of the selected study specimens, and their methylation status (plus that of *MLH1*) was determined by COBRA in CRC specimens positive for the methylation of the *MLH1* promoter ($n = 8$), their paired normal colon tissue samples, and CRC specimens negative for *MLH1* methylation ($n = 8$). Each column represents a clinical specimen (ID numbers are shown), and each row indicates a gene corresponding to an MCA–RDA product. Red box, methylated gene; blue box, unmethylated gene; white box, not examined.

fragments thus appeared to be specific to the cancerous state with a slightly increased prevalence among *MLH1* methylation-positive CRC.

The fragments in the third group (*MGC29643* to *IMAGE5728979*) were methylated in <25% both of normal specimens and of cancer specimens negative for *MLH1* methylation. The methylation of these genes thus appears to be regulated in concert with that of *MLH1*.

Analysis of BMP3

Among the genomic clones analyzed, we first focused on that corresponding to BMP3. BMP3 is a member of the transforming growth factor-β (TGF-β) superfamily of proteins that also includes TGF-β1, TGF-β2, TGF-β3, Mullerian inhibitory substance, BMP2A, BMP2B, BMP6, growth-differentiation factor (GDF) 5, GDF6 and GDF7 (17,18). Members of this protein superfamily exert inhibitory effects on various human cancers through activation of their cognate receptors and SMAD proteins (19,20). BMP2, for instance, induces both the activation of the p38 isoform of mitogen-activated protein kinase and apoptosis in medulloblastoma cells (21). Although little is known of the physiological functions of BMP3, it is possible that this protein also possesses antitumor activity and that its expression is epigenetically regulated in cancer cells. Interestingly, Dai *et al.* (22) have recently reported that *BMP3* promoter is methylated frequently (~50%) in non-small-cell lung carcinoma, which many imply that dysfunction of BMP3 may be commonly involved in the carcinogenesis of a wide range of human tumors.

The COBRA assay revealed that the MCA–RDA clone corresponding to the promoter region of *BMP3* was methylated in CRC specimens that were positive or negative for *MLH1* methylation (Figures 1 and 2A). Further, as shown in Figure 2B, detailed analysis of the methylation status of the *BMP3* promoter by sequencing of DNA fragments after sodium bisulfite treatment revealed extensive hemi- or biallelic methylation of the promoter in CRC specimens positive for *MLH1* methylation (ID nos 225, 318 and 481) but not in one negative for *MLH1* methylation (ID no. 249). CpG methylation throughout the promoter fragment was also evident in CRC cell lines positive (HCT116) or negative (Caco2) for *MLH1* methylation, but not in the *MLH1* methylation-negative line SW480. Together with the COBRA data in Figure 1, these results suggest that the promoter region of *BMP3* is methylated in all clinical specimens and cell lines positive for methylation of the *MLH1* promoter as well as in some specimens and cell lines negative for *MLH1* methylation.

We then examined whether the epigenetic changes in the *BMP3* promoter affected its transcriptional activity. Quantitative real-time RT–PCR analysis revealed that *BMP3*

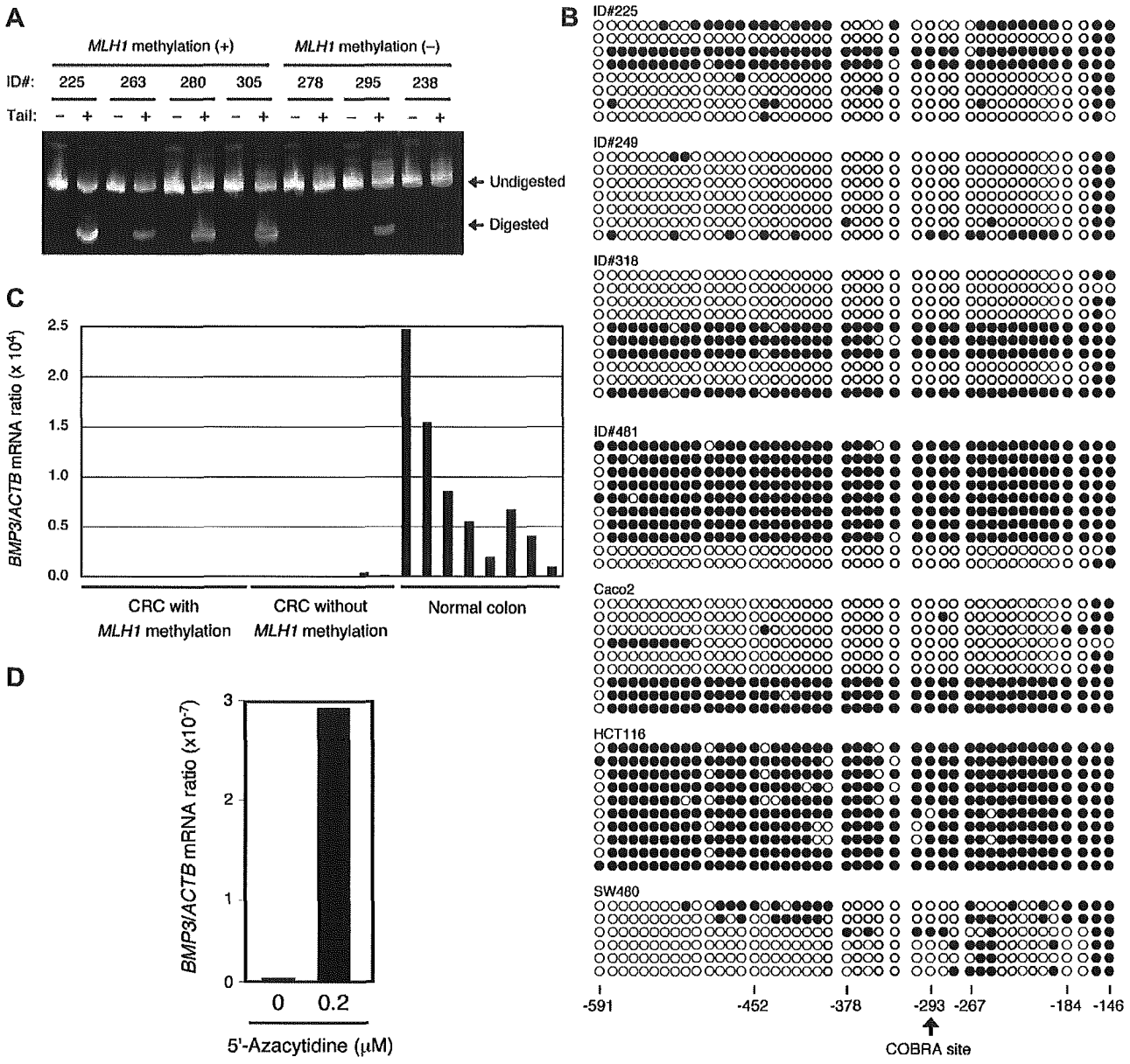

Fig. 2. Methylation status of the *BMP3* promoter and *BMP3* expression in CRC specimens. (**A**) The methylation status of the promoter region of *BMP3* in the indicated clinical specimens was examined by COBRA. Sensitivity of PCR products to digestion with TaiI is indicative of methylation of the CpG island examined. (**B**) Genomic DNA of the indicated clinical specimens and CRC cell lines (Caco2, HCT116 and SW480) was treated with sodium bisulfite, after which the *BMP3* promoter region was amplified by PCR and sequenced. Closed and open circles indicate methylated and unmethylated CpG islands, respectively. The nucleotide positions of the CpG islands (numbered relative to the transcriptional start site) are indicated at the bottom, and the TaiI digestion site for COBRA in (A) is shown by the arrow. (**C**) The level of expression of *BMP3* relative to that of *ACTB* in clinical specimens was determined by quantitative RT–PCR. (**D**) HCT116 cells were incubated for 72 h with or without 0.2 μM of 5′-azacytidine, and were then subjected to RT–PCR analysis for determination of the amount of *BMP3* mRNA relative to that of *ACTB* mRNA.

was transcriptionally silent in CRC specimens positive for *MLH1* methylation (Figure 2C), in which the *BMP3* promoter was also extensively methylated. In contrast, *BMP3* mRNA was abundant in the paired normal colon tissue samples. Although *BMP3* expression was detected in some CRC specimens negative for *MLH1* methylation, the level of expression was greatly reduced compared with that in normal colon tissue. These data thus indicate that *BMP3* transcription is suppressed in most CRCs.

In order to directly examine the relationship between promoter methylation and gene silencing of *BMP3*, HCT116 cells were incubated for 3 days with 5′-azacytidine, an inhibitor of *de novo* methylation of genomic DNA. Interestingly, treatment with 5′-azacytidine markedly induced the amount of *BMP3* mRNA in the cells (Figure 2D) and demethylation of its promoter region as well (data not shown). Therefore, extensive methylation of the *BMP3* promoter region should be directly linked to the suppression of its transcription.

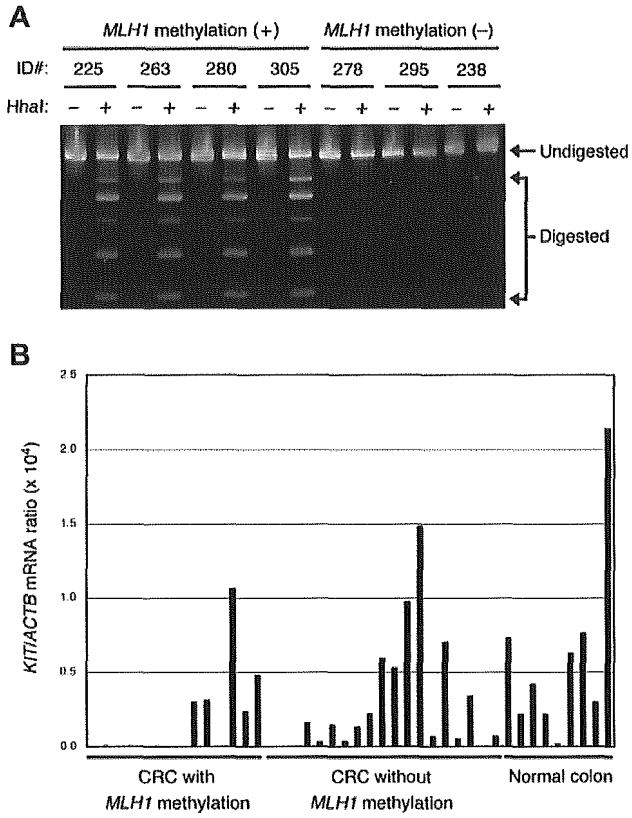

Fig. 3. *Methylation status of the KIT promoter and KIT expression in CRC specimens.* (**A**) The methylation status of the promoter region of *KIT* in the indicated clinical specimens was examined by COBRA. Sensitivity of PCR products to digestion with HhaI is indicative of methylation of the CpG island examined. (**B**) The level of expression of *KIT* relative to that of *ACTB* in clinical specimens was determined by quantitative RT–PCR.

Analysis of KIT

KIT encodes a receptor tyrosine kinase for stem cell factor. Point mutations in *KIT* that increase the kinase activity of the encoded protein have been identified in human gastrointestinal stromal tumors (23), suggestive of a causative role for KIT in these tumors. The expression and activation status of KIT in CRCs have been unclear, however (24,25). We therefore analyzed the methylation status of the *KIT* promoter region in our samples.

Methylation of the *KIT* promoter was highly restricted to CRC specimens positive for *MLH1* methylation (Figures 1 and 3A). However, the abundance of *KIT* mRNA did not necessarily match the methylation status of the *KIT* promoter. Despite extensive methylation of the promoter in one CRC sample (ID no.77), for instance, the amount of *KIT* mRNA was relatively high (*KIT/ACTB* mRNA ratio = 4.78×10^{-5}), indicating that promoter methylation might not be a major determinant of transcriptional activity. It is possible, however, that our COBRA analysis revealed the methylation status of a CpG site that is not important for *KIT* transcription.

The mean expression level of *KIT* in the *MLH1* methylation-positive CRC specimens [*KIT/ACTB* mRNA ratio, $1.72 \times 10^{-5} \pm 3.02 \times 10^{-5}$ (mean ± SD)] was significantly lower than that in normal colon tissue ($6.03 \times 10^{-5} \pm 6.29 \times 10^{-5}$; $P = 0.038$, Student's *t*-test). The level of *KIT* expression in CRCs negative for *MLH1* methylation ($2.92 \times 10^{-5} \pm 1.61 \times 10^{-5}$) was also lower than that in normal colon tissue, but this difference was not significant ($P = 0.123$). It is therefore likely that *KIT* is not overexpressed in CRCs.

Discussion

We have screened for genomic fragments whose CpG islands are selectively methylated in CRC specimens positive for methylation of the *MLH1* promoter region. We could readily identify hundreds of genomic fragments with CpG islands that were expected to be differentially methylated between CRCs with or without *MLH1* methylation. Twenty-eight such clones (Table II) were indeed proved to be preferentially methylated in the four CRC specimens positive for *MLH1* methylation compared with the four samples negative for *MLH1* methylation, both of which were used in the original MCA–RDA screening (data not shown).

To verify the selective methylation of these clones, we performed COBRA with a different set of specimens including eight CRCs with *MLH1* methylation and their paired normal tissue samples as well as eight CRCs without *MLH1* methylation. Although all the 28 clones examined were preferentially methylated in the CRC specimens positive for *MLH1* methylation, their methylation profiles among the specimens were not identical, indicating that all CpG methylation observed in MSI-positive CRCs was not specific to this subtype of tumor.

The methylation of certain genomic fragments (14 out of 28 clones examined), however, was highly specific to CRCs that manifested *MLH1* methylation. Almost 50% of the genes were thus methylated in a parallel manner to the CpG methylation of the *MLH1* gene, indicating that a subset of genes is specifically methylated in a subset of CRCs. Our data thus support the existence of CIMP-positive CRCs (14), while it would be mandatory for the better characterization of CIMP-positive tumors to further collect co-methylated genes and to define precisely the hallmark genes for the identification of CIMP (26). It would be interesting to examine whether such clearly defined CIMP is associated with certain clinical manifestations.

Genes corresponding to the co-methylated genomic fragments in our assay included those whose function relates to cell proliferation or differentiation. The predicted structure of NELL2, for example, contains epidermal growth factor (EGF)-like repeats (27), which are present in diverse proteins involved in regulation of the cell cycle, cell proliferation, and developmental processes. NTAK is a member of the EGF family of proteins and is a ligand and activator of ErbB protein tyrosine kinases (28). In addition, GDF7 is a member of the TGF-β superfamily (18), and *TCF7L1* is highly homologous to TCF1 which is a target gene of the Wnt-β-catenin signaling pathway (29), and which plays an important role in CRC carcinogenesis. Aberrant epigenetic regulation of these genes may thus contribute to the pathogenesis or clinical features of CRCs positive for *MLH1* methylation.

The MCA–RDA method thus proved to be highly effective for the identification of differentially methylated genes among fresh clinical specimens. Given the high fidelity of this approach, it is likely that a large number of genes (or genomic fragments) are methylated in CRCs in concert with methylation of the *MLH1* promoter. Our study provides a basis for further characterization of the molecular pathogenesis of CRCs classified as MSI. Together with the results of other

studies (7,30), it also suggests the possibility of development of a stratification scheme for CRCs based on genome methylation profile.

Supplementary material

Supplementary material can be found at: http://www.carcin.oxfordjournals.org/

Acknowledgements

This study was supported by a Grant-in-Aid for Third-Term Comprehensive Control Research for Cancer from the Ministry of Health, Labor, and Welfare of Japan, and by a grant for 'High-Tech Research Center' Project for Private Universities: Matching Fund Subsidy (2002–2006) from the Ministry of Education, Culture, Sports, Science, and Technology of Japan.

Conflict of Interest Statement: None declared.

References

1. Lengauer,C., Kinzler,K.W. and Vogelstein,B. (1998) Genetic instabilities in human cancers. *Nature*, **396**, 643–649.
2. Kinzler,K.W. and Vogelstein,B. (1996) Lessons from hereditary colorectal cancer. *Cell*, **87**, 159–170.
3. Ionov,Y., Peinado,M.A., Malkhosyan,S., Shibata,D. and Perucho,M. (1993) Ubiquitous somatic mutations in simple repeated sequences reveal a new mechanism for colonic carcinogenesis. *Nature*, **363**, 558–561.
4. Fishel,R., Lescoe,M.K., Rao,M.R., Copeland,N.G., Jenkins,N.A., Garber,J., Kane,M. and Kolodner,R. (1993) The human mutator gene homolog *MSH2* and its association with hereditary non-polyposis colon cancer. *Cell*, **75**, 1027–1038.
5. Bronner,C.E., Baker,S.M., Morrison,P.T. *et al.* (1994) Mutation in the DNA mismatch repair gene homologue *hMLH1* is associated with hereditary non-polyposis colon cancer. *Nature*, **368**, 258–261.
6. Papadopoulos,N., Nicolaides,N.C., Wei,Y.F. *et al.* (1994) Mutation of a mutL homolog in hereditary colon cancer. *Science*, **263**, 1625–1629.
7. Toyota,M., Ahuja,N., Ohe-Toyota,M., Herman,J.G., Baylin,S.B. and Issa,J.P. (1999) CpG island methylator phenotype in colorectal cancer. *Proc. Natl Acad. Sci. USA*, **96**, 8681–8686.
8. Miyakura,Y., Sugano,K., Konishi,F., Ichikawa,A., Maekawa,M., Shitoh,K., Igarashi,S., Kotake,K., Koyama,Y. and Nagai,H. (2001) Extensive methylation of h*MLH1* promoter region predominates in proximal colon cancer with microsatellite instability. *Gastroenterology*, **121**, 1300–1309.
9. Cunningham,J.M., Christensen,E.R., Tester,D.J., Kim,C.Y., Roche,P.C., Burgart,L.J. and Thibodeau,S.N. (1998) Hypermethylation of the h*MLH1* promoter in colon cancer with microsatellite instability. *Cancer Res.*, **58**, 3455–3460.
10. Veigl,M.L., Kasturi,L., Olechnowicz,J. *et al.* (1998) Biallelic inactivation of h*MLH1* by epigenetic gene silencing, a novel mechanism causing human MSI cancers. *Proc. Natl Acad. Sci. USA*, **95**, 8698–8702.
11. Koinuma,K., Shitoh,K., Miyakura,Y. *et al.* (2004) Mutations of BRAF are associated with extensive h*MLH1* promoter methylation in sporadic colorectal carcinomas. *Int. J. Cancer*, **108**, 237–242.
12. Wang,L., Cunningham,J.M., Winters,J.L., Guenther,J.C., French,A.J., Boardman,L.A., Burgart,L.J., McDonnell,S.K., Schaid,D.J. and Thibodeau,S.N. (2003) BRAF mutations in colon cancer are not likely attributable to defective DNA mismatch repair. *Cancer Res.*, **63**, 5209–5212.
13. Oliveira,C., Pinto,M., Duval,A. *et al.* (2003) BRAF mutations characterize colon but not gastric cancer with mismatch repair deficiency. *Oncogene*, **22**, 9192–9196.
14. Issa,J.P. (2004) Opinion: CpG island methylator phenotype in cancer. *Nat. Rev. Cancer*, **4**, 988–993.
15. Toyota,M., Ho,C., Ahuja,N., Jair,K.W., Li,Q., Ohe-Toyota,M., Baylin,S.B. and Issa,J.P. (1999) Identification of differentially methylated sequences in colorectal cancer by methylated CpG island amplification. *Cancer Res.*, **59**, 2307–2312.
16. Xiong,Z. and Laird,P.W. (1997) COBRA: a sensitive and quantitative DNA methylation assay. *Nucleic Acids Res.*, **25**, 2532–2534.
17. Hogan,B.L. (1996) Bone morphogenetic proteins: multifunctional regulators of vertebrate development. *Genes Dev.*, **10**, 1580–1594.
18. Davidson,A.J., Postlethwait,J.H., Yan,Y.L., Beier,D.R., van Doren,C., Foernzler,D., Celeste,A.J., Crosier,K.E. and Crosier,P.S. (1999) Isolation of zebrafish gdf7 and comparative genetic mapping of genes belonging to the growth/differentiation factor 5, 6, 7 subgroup of the TGF-beta superfamily. *Genome Res.*, **9**, 121–129.
19. Miyazono,K., Kusanagi,K. and Inoue,H. (2001) Divergence and convergence of TGF-beta/BMP signaling. *J. Cell. Physiol.*, **187**, 265–276.
20. Bottinger,E.P., Jakubczak,J.L., Haines,D.C., Bagnall,K. and Wakefield,L.M. (1997) Transgenic mice overexpressing a dominant-negative mutant type II transforming growth factor beta receptor show enhanced tumorigenesis in the mammary gland and lung in response to the carcinogen 7,12-dimethylbenz-[a]-anthracene. *Cancer Res.*, **57**, 5564–5570.
21. Hallahan,A.R., Pritchard,J.I., Chandraratna,R.A., Ellenbogen,R.G., Geyer,J.R., Overland,R.P., Strand,A.D., Tapscott,S.J. and Olson,J.M. (2003) BMP-2 mediates retinoid-induced apoptosis in medulloblastoma cells through a paracrine effect. *Nat. Med.*, **9**, 1033–1038.
22. Dai,Z., Popkie,A.P., Zhu,W.G. *et al.* (2004) Bone morphogenetic protein 3B silencing in non-small-cell lung cancer. *Oncogene*, **23**, 3521–3529.
23. Hirota,S., Isozaki,K., Moriyama,Y. *et al.* (1998) Gain-of-function mutations of c-kit in human gastrointestinal stromal tumors. *Science*, **279**, 577–580.
24. Bellone,G., Silvestri,S., Artusio,E., Tibaudi,D., Turletti,A., Geuna,M., Giachino,C., Valente,G., Emanuelli,G. and Rodeck,U. (1997) Growth stimulation of colorectal carcinoma cells via the c-kit receptor is inhibited by TGF-beta 1. *J. Cell. Physiol.*, **172**, 1–11.
25. Sammarco,I., Capurso,G., Coppola,L. *et al.* (2004) Expression of the proto-oncogene c-KIT in normal and tumor tissues from colorectal carcinoma patients. *Int. J. Colorectal Dis.*, **19**, 545–553.
26. Yamashita,K., Dai,T., Dai,Y., Yamamoto,F. and Perucho,M. (2003) Genetics supersedes epigenetics in colon cancer phenotype. *Cancer Cell*, **4**, 121–131.
27. Watanabe,T.K., Katagiri,T., Suzuki,M., Shimizu,F., Fujiwara,T., Kanemoto,N., Nakamura,Y., Hirai,Y., Maekawa,H. and Takahashi,E. (1996) Cloning and characterization of two novel human cDNAs (NELL1 and NELL2) encoding proteins with six EGF-like repeats. *Genomics*, **38**, 273–276.
28. Higashiyama,S., Horikawa,M., Yamada,K. *et al.* (1997) A novel brain-derived member of the epidermal growth factor family that interacts with ErbB3 and ErbB4. *J. Biochem.*, **122**, 675–680.
29. Castrop,J., van Norren,K. and Clevers,H. (1992) A gene family of HMG-box transcription factors with homology to TCF-1. *Nucleic Acids Res.*, **20**, 611.
30. Toyota,M., Ohe-Toyota,M., Ahuja,N. and Issa,J.P. (2000) Distinct genetic profiles in colorectal tumors with or without the CpG island methylator phenotype. *Proc. Natl Acad. Sci. USA*, **97**, 710–715.

Received April 29, 2005; revised July 10, 2005; accepted July 12, 2005

THE JOURNAL OF BIOLOGICAL CHEMISTRY
Vol. 280, No. 13, Issue of April 1, pp. 12621–12629, 2005
Printed in U.S.A.

Signal Transducers and Activators of Transcription 3 Augments the Transcriptional Activity of CCAAT/Enhancer-binding Protein α in Granulocyte Colony-stimulating Factor Signaling Pathway*

Received for publication, July 26, 2004, and in revised form, January 3, 2005
Published, JBC Papers in Press, January 21, 2005, DOI 10.1074/jbc.M408442200

Akihiko Numata‡, Kazuya Shimoda‡§, Kenjiro Kamezaki‡, Takashi Haro‡, Haruko Kakumitsu‡, Koutarou Shide‡, Kouji Kato‡, Toshihiro Miyamoto‡, Yoshihiro Yamashita¶, Yasuo Oshima‖, Hideaki Nakajima, Atsushi Iwama‡‡, Kenichi Aoki‡, Ken Takase‡, Hisashi Gondo‡, Hiroyuki Mano¶, and Mine Harada‡**

*From the ‡Medicine and Biosystemic Science, Kyushu University Graduate School of Medical Sciences, 3-1-1 Maidashi, Higashi-ku, Fukuoka, Fukuoka, 812-8582, the ¶Division of Functional Genomics, Jichi Medical School, 3311-1 Yakushiji, Kawaguchi-gun, Tochigi, 329-0498, the ‖Department of Clinical Pharmacology, Jichi Medical School, 3311-1 Yakushiji, Kawaguchi-gun, Tochigi, 329-0498, the **Department of Hematopoietic Factors, Institute of Medical Science, University of Tokyo, 4-6-1 Shirokanedai, Minato-ku, Tokyo, 108-8639, and the ‡‡Laboratory of Stem Cell Therapy, Center for Experimental Medicine, Institute of Medical Science, University of Tokyo, 4-6-1 Shirokanedai, Minato-ku, Tokyo, 108-8639, Japan*

The Janus kinase (Jak)-Stat pathway plays an essential role in cytokine signaling. Granulocyte colony-stimulating factor (G-CSF) promotes granulopoiesis and granulocytic differentiation, and Stat3 is the principle Stat protein activated by G-CSF. Upon treatment with G-CSF, the interleukin-3-dependent cell line 32D clone 3(32Dcl3) differentiates into neutrophils, and 32Dcl3 cells expressing dominant-negative Stat3 (32Dcl3/DNStat3) proliferate in G-CSF without differentiation. Gene expression profile and quantitative PCR analysis of G-CSF-stimulated cell lines revealed that the expression of *C/EBPα* was up-regulated by the activation of Stat3. In addition, activated Stat3 bound to CCAAT/enhancer-binding protein (C/EBP)α, leading to the enhancement of the transcription activity of C/EBPα. Conditional expression of C/EBPα in 32Dcl3/DNStat3 cells after G-CSF stimulation abolishes the G-CSF-dependent cell proliferation and induces granulocytic differentiation. Although granulocyte-specific genes, such as the G-CSF receptor, lysozyme M, and neutrophil gelatinase-associated lipocalin precursor (*NGAL*) are regulated by Stat3, only NGAL was induced by the restoration of C/EBPα after stimulation with G-CSF in 32Dcl3/DNStat3 cells. These results show that one of the major roles of Stat3 in the G-CSF signaling pathway is to augment the function of C/EBPα, which is essential for myeloid differentiation. Additionally, cooperation of C/EBPα with other Stat3-activated proteins are required for the induction of some G-CSF responsive genes including lysozyme M and the G-CSF receptor.

The proliferation and differentiation of hematopoietic progenitor cells are regulated by cytokines (1). Among these, granulocyte colony-stimulating factor (G-CSF)[1] specifically stimulates cells that are committed to the myeloid lineage (2). The importance of G-CSF to the regulation of granulopoiesis has been confirmed by the observation of severe neutropenia in mice carrying homozygous deletions of their G-CSF or G-CSF receptor genes (3, 4). Cytokines activate several intracellular signaling pathways, and the Janus kinase (Jak) signal transducers and activators of transcription (Stat) pathway is essential for cytokine function (5, 6). The binding of G-CSF to cell surface G-CSF receptors activates Jak1, Jak2, and Tyk2 followed by the activation of Stat1, Stat3, and Stat5 (7–9). Stat3 is the principle protein activated by G-CSF (8, 10). Phosphorylated Stats translocate from the cytoplasm into the nucleus and induce transcription of their target genes within a short period of time. 32Dcl3 cells differentiate to neutrophils following treatment with G-CSF. In contrast to their parental cells, 32Dcl3 cells expressing dominant-negative Stat3 (32Dcl3/DNStat3) proliferate in the presence of G-CSF, but they maintain immature morphologic characteristics without evidence of differentiation (11). Additionally, transgenic mice with a targeted mutation of their G-CSF receptor that abolishes G-CSF-dependent Stat3 activation show severe neutropenia with an accumulation of immature myeloid precursors in their bone marrows (12). To clarify the role of Stat3 in the G-CSF signaling pathway, we wished to identify target genes of Stat3.

We found that the levels of CCAAT/enhancer-binding protein (C/EBP) α mRNA were up-regulated following G-CSF stimulation in 32Dcl3 but were unchanged in 32Dcl3/DNStat3. In addition, the activation of Stat3 augmented the function of C/EBPα, which is the essential transcriptional factor for myeloid differentiation. G-CSF-induced granulocytic differentiation was restored in 32Dcl3/DNStat3 cells by the conditional expression of C/EBPα. These results show that one of the major

* This work was supported by a grant of the Japan Leukemia Research Foundation (2002) and Grants-in-aid for Scientific Research 11307015 and 15390302 from the Ministry of Education, Science, Sports, and Culture in Japan. The costs of publication of this article were defrayed in part by the payment of page charges. This article must therefore be hereby marked "*advertisement*" in accordance with 18 U.S.C. Section 1734 solely to indicate this fact.

§ To whom correspondence should be addressed. Tel.: 81-92-642-5230; Fax: 81-92-642-5247; E-mail: kshimoda@intmed1.med.kyushu-u.ac.jp.

[1] The abbreviations used are: G-CSF, granulocyte colony-stimulating factor; IL, interleukin; C/EBPα, CCAAT/enhancer-binding protein; NGAL, neutrophil gelatinase-associated lipocalin precursor; Jak, Janus kinase; Stat, signal transducers and activators of transcription; DNStat3, dominant-negative Stat3; IRES, internal ribosome entry site; GFP, green fluorescent protein; ER, endoplasmic reticulum; IFN, interferon; PBS, phosphate-buffered saline; GAPDH, glyceraldehyde-3-phosphate dehydrogenase; FACS, fluorescence-activated cell sorter; LUC, luciferase; ERK, extracellular signal-regulated kinase; MAP, mitogen-activated protein; TK, thymidine kinase; 4-HT, 4-hydroxytamoxifen.

roles of Stat3 in the G-CSF signaling pathway is to enhance the function of C/EBPα.

MATERIALS AND METHODS

Cell Culture, Expression Plasmid, and Cytokines—32D clone 3 (32Dcl3) and 32Dcl3/DNStat3 cells (DNStat3 deletes the transactivation domain of Stat3) were cultured in RPMI 1640 supplemented with 10% heat-inactivated fetal bovine serum (ICN, Osaka, Japan), penicillin/streptomycin (Invitrogen), recombinant murine interleukin-3 (IL-3) (Kirin Brewery, Takasaki, Japan), and recombinant human G-CSF (Chugai Pharmaceutical, Tokyo, Japan). 293T cells were cultured in Dulbecco's modified Eagle's medium containing 10% fetal bovine serum, penicillin/streptomycin, and L-glutamine.

For the construction of pTag2A-G-CSF receptor, the human G-CSF receptor cDNA (13) (pHQ3, kindly provided by S. Nagata and R. Fukunaga) was excited from the pBluescipt vector and inserted into the FLAG-tagged mammalian expression plasmid pCMV-Tag2A (Clontech). pcDNA3-rat C/EBPα was described before (14). Stat3 cDNA was amplified by PCR and inserted into pCMV-HA vector (Clontech). Stat3c cDNA was elicited from RCMV-Stat3c (15), kindly given from Dr. Darnell, and inserted into pcDNA3.1 (Clontech). For the construction of pMY-IRES-GFP/C/EBPα-ER, full-length human C/EBPα cDNA was fused in-frame with ligand-binding domain (amino acids 281–599) of mouse estrogen receptor harboring a mutation (G525R) that confers selective responsiveness to 4-hydroxytamoxifen (4-HT). A reporter construct of a minimal TK promoter with CEBP-binding sites (p(C/EBP)2TK) was described previously (14).

Murine recombinant leukemia inhibitory factor, natural IFN-α, and recombinant IFN-γ were purchased from Sigma, HyCult Biotechnology (Uden, The Netherlands), and Peprotech (Rocky Hill, NJ), respectively. For Western blotting, 32Dcl3 cells or 32Dcl3/DNStat3 cells were deprived of IL-3 for 12 h. Then cells were stimulated with G-CSF (10 ng/ml), IL-3 (10 ng/ml), leukemia inhibitory factor (10 ng/ml), IFN-α (1,000 units/ml), or IFN-γ (1,000 units/ml) for 30 min.

Microarray Analysis—32D cl3 and 32Dcl3/DNStat3 cells maintained in IL-3 were washed twice with PBS and starved of cytokine in RPMI 1640 containing 10% fetal bovine serum for 8 h and then stimulated with 10 ng/ml G-CSF. Total RNA was extracted, by the acid guanidinium method, from 32Dcl3 and 32Dcl3/DNStat3 cells before or after the stimulation for 2 h with G-CSF. Double-stranded cDNA synthesized from the total RNA (20 μg/sample) was then used to prepare biotin-labeled cRNA for the hybridization with GeneChip MGU74Avs2 microarrays (Affymetrix, Santa Clara, CA) harboring oligonucleotides corresponding to ~6000 known genes as well as ~6000 expressed sequence tag sequences. Hybridization, washing, and detection of signals on the arrays were performed with the GeneChip system (Affymetrix).

Quantitative Real-time Reverse Transcription-PCR Assay—32Dcl3 and 32Dcl3/DNStat3 cells maintained in IL-3, were washed twice with PBS and starved of cytokines for 8 h and then stimulated with 10 ng/ml G-CSF. Cells were harvested at the indicated times, and total RNA was isolated using Isogen (Nippon gene, Tokyo, Japan) according to the manufacturer's instructions. One microgram of extracted RNA was transcribed in a 20-μl cDNA synthesis reaction using an RNA PCR kit (AMV) (Takara, Tokyo, Japan). Real-time PCR for C/EBPα, G-CSF receptor, lysozyme M, neutrophil gelatinase-associated lipocalin precursor (NGAL), and glyceraldehyde 3-phosphate dehydrogenase (GAPDH) was performed by a TaqMan assay on an ABI 7000 system. PCR primers and probes were designed as follows: murine C/EBPα, sense, 5′-CCA TGT GGT AGG AGA CAG AGA CCT A-3′, and antisense, 5′-CTC TGG GAT GGA TCG ATT GTG-3′; probe FAM-5′-CGG CTG GCG ACA TAC AGT ACA CAC AAG-3′-TAMRA, and sense, 5′-CCA AGA AGT CGG TGG ACA AGA-3′, and antisense, 5′-CGG TCA TTG TCA CTG GTC AAC T-3′; probe FAM-5′-AGC ACC TTC TGT TGC GTC TCC ACG TT-3′-TAMRA; murine G-CSF receptor, sense, 5′-CTA AAC ATC TCC CTC CAT GAC TT-3′, and antisense, 5′-GGC CAT GAG GTA GAC ATG ATA CAA-3′; probe FAM-5′-CAT CTT CTC TGT CCC CAC CGA CCA A-3′-TAMRA; murine lysozyme M, sense, 5′-TGC CTG TGG GAT CAA TTG C-3′, and antisense, 5′-ATG CCA CCC ATG CTC GAA T-3′; probe 5′-FAM-CAG TGA TGT CAT CCT GCA GAC CA-TAMRA-3′; murine NGAL, sense, 5′-GGC CTC AAG GAC GAC AAC A-3′, and antisense, 5′-CAC CAC CCA TTC AGT TGT CAA T-3′; probe 5′-FAM-CAT CTT CTC TGT CCC CAC CGA CCA A-TAMRA-3′, and murine GAPDH sense, 5′-ACG GCA AAT TCA ACG GCA-3′, and antisense, 5′-AGA TGG TGA TGG GCT TCC-3′; probe 5′-FAM-AGG CCG AGA ATG GGA AGC TTG TCA TC-TAMRA-3′. PCR amplifications were performed in a 50-μl volume, containing 4 μl of cDNA template, 50 mM KCl, 10 mM Tris-HCl(pH 8.3), 10 mM EDTA, 60 nM, 200 μM dNTPs, 3 mM $MgCl_2$, 200 nM each primer, 0.625 units of AmpliTaqGold, and 0.25 units of AmpErase uracil *N*-glycosylase. Each amplification reaction also contained 100 nM appropriate detection probe. Each PCR amplification was performed in duplicate, using conditions of 50 °C for 2 min preceding 95 °C for 10 min followed by 40 cycles of amplification (95 °C for 15 s, 60 °C for 1 min). In each reaction, GAPDH was amplified as a housekeeping gene to calculate a standard curve and allow for the correction for variations in target sample quantities. Relative copy numbers were calculated for each sample from the standard curve after normalization to GAPDH by the instrument software.

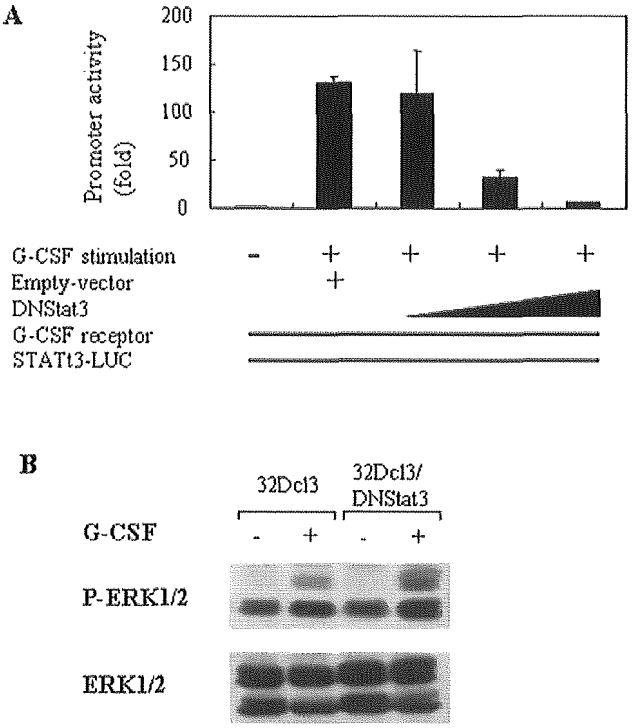

FIG. 1. **The effect of dominant-negative Stat3 on G-CSF signaling pathway.** *A*, transient transfection in 293T cells with a reporter construct with α2-macroglobulin promoter (*STAT13-LUC*), dominant-negative Stat3, and G-CSF receptor. Twelve hours after transfection, cells were stimulated with 10 ng/ml G-CSF. Promoter activity was measured as luciferase activity 36 h after transfection. The *vertical axis number* is the fold induction when compared with control. *B*, 32Dcl3 cells or 32Dcl3/DNStat3 cells were cultured with IL-3 and then deprived of IL-3 for 12 h. Cells were treated with the G-CSF for 30 min and lysed. Post-nuclear supernatants were resolved by 10% SDS-PAGE and transferred to nitrocellulose membranes. Membranes were probed using the indicated antibodies. *p-ERK1/2*, phosphorylated ERK1/2.

Conditional C/EBPα Expression—pMY-IRES-GFP/C/EBPα-ER was transfected into 32Dcl3 and 32Dcl3/DNStat3 cells by electroporation. 5×10^6 cells were transfected with 20 μg of expression vector, and GFP-positive cells were sorted by FACS Vantage (BD Biosciences). Expression of C/EBPα was determined by Western blotting analysis (see below).

Luciferase Assay—293T cells were transfected by the calcium phosphate precipitation method in 6-well plates, and luciferase activity was assayed using a luminometer Lumat LB9507 (Berthold Technologies, Bad Wildbad, Germany) according to the manufacturer's protocol. Each expression plasmid amount was 50–100 ng/well, and the same amount of empty expression vector was used as control, respectively. Results of reporter assays represent the average values for relative luciferase activity generated from five independent experiments.

Flow Cytometry—1×10^7 cells were incubated with 5 μl of recombinant phosphatidylethanolamine-conjugated rabbit anti-murine Gr1 monoclonal antibody (BD Biosciences) for 30 min at 4 °C, washed twice in PBS, and analyzed on a FACS Calibur (BD Biosciences).

Immunoprecipitation and Immunoblotting—Cells were lysed with lysis buffer, and lysates were immunoprecipitated with anti C/EBPβ (Santa Cruz Biotechnology, Santa Cruz, CA) as described previously (8). Total cell lysates or the immunoprecipitates were resolved by 10% SDS-PAGE and transferred to a nitrocellulose membrane. Membranes

TABLE I
Microarray analysis

32Dcl3 and 32Dcl3/DNStat3 cells were starved of cytokines for 8 h and then stimulated or left unstimulated with 10 ng/ml G-CSF. Total RNA was extracted from each fraction and was subjected to the hybridization with high-density oligonucleotide microarrays (MGU74Av2). Fold induction means a rate of increase in gene expression level by G-CSF stimulation. Candidate genes were identified as transcripts that were up-regulated in 32Dcl3 cells and down-regulated or unchanged in 32Dcl3/DNStat3 cells after G-CSF stimulation.

Gene product name	Abbreviation	Accession number	Fold induction	
			32Dcl3	32Dcl3/DNStat3
B-cell leukemia/lymphoma α	Bcl2	L31532	35.6	0.0629
CyclinE1	*Ccne1*	NM007633	29.7	0.690
Serotonin-gated ion channel	*5HT3*	M74425	27.2	0.592
KIF3B protein	*kif3b*	D26077	21.5	0.921
Protein kinase, serine/arginine-specific 1	*Srpk1*	AB012290	18.7	0.321
MAP kinase-interacting serine/threonine kinase 1	*Mknk1*	Y11091	15.7	0.845
Protein tyrosine phosphatase	*Ptpn13*	D83966	12.4	0.964
Transferrin receptor	*Trfr*	X57349	10.6	0.964
Lymphocyte antigen 57	*Ly57*	AF068182	9.62	0.968
Macrophage stimulating 1 receptor	*Mst1r*	X74736	8.83	0.762
Mitogen-activated protein kinase kinase 7	*MKK7*	AB005654	8.14	0.980
RAR-related orphan receptor alpha	*Rora*	U53228	7.94	0.861
Hemoglobin Y, β-like embryonic chain	*Hbb-y*	V00726	7.38	0.375
Runt related transcription factor 1	*Runx1*	NM009821	7.01	0.226
Microtubule-associated protein 6	*Mtap6*	Y14754	5.06	0.885
CCAAT/enhancer binding protein α	*C/EBPα*	M62362	2.05	0.840
Ecotoropic viral integration site 1	Evi1	M21829	1.55	0.239
Integrin alpha L	*Itgal*	M60778	1.35	0.567
Ninjurin 1	*Ninj1*	U91513	1.34	0.783
Interleukin 17 receptor	*IL17R*	U31993	1.24	0.449
Mucosal addressin	*MAdCAM*	D50434	1.14	0.527
Carbon catabolite repression 4 homolog	*Ccr4*	X16670	1.06	0.0768
Friend leukemia integration 1	*Fli1*	X59421	1.01	0.305

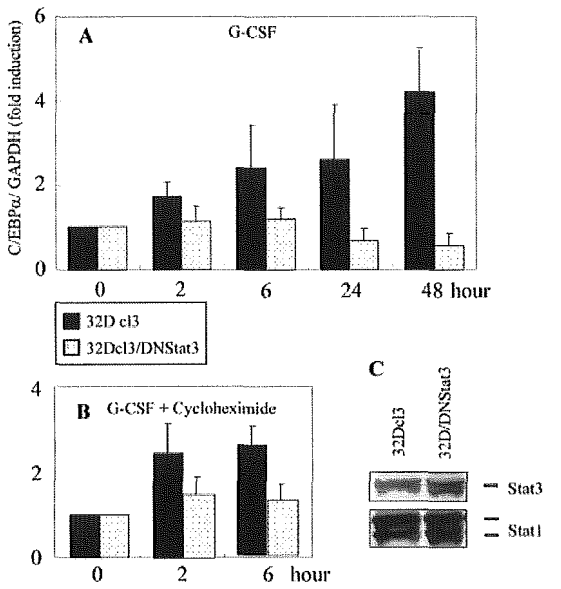

FIG. 2. **Expression of C/EBPα mRNA in G-CSF-stimulated 32Dcl3 and 32Dcl3/DNStat3 cells.** *A* and *B*, 32Dcl3 and 32Dcl3/DNStat3 cells maintained in IL-3 were washed twice with PBS and starved of cytokines for 8 h and stimulated with 10 ng/ml G-CSF (*A*) or 10 ng/ml G-CSF and 10 μg/ml cycloheximide (*B*). Total RNA was isolated from both cell lines at the indicated times and transcribed to cDNA, which was subjected to real-time PCR for murine C/EBPα. The *numbers* given on the *vertical axis* represent the fold induction of the ratios of GAPDH-normalized expression values when compared with those before G-CSF stimulation. Results are expressed as mean fold of two independent experiments.

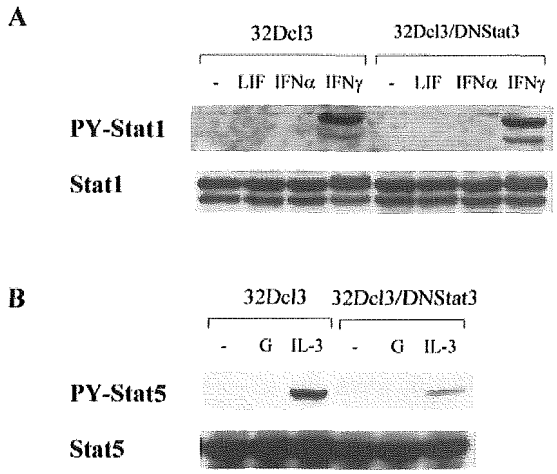

FIG. 3. **The effect of the abrogation of Stat3 on other cytokine signaling pathway.** 32Dcl3 cells or 32Dcl3/DNStat3 cells were cultured with IL-3 and then deprived of IL-3 for 12 h. Cells were treated with the indicated cytokines for 30 min and lysed. Post-nuclear supernatants were resolved by 10% SDS-PAGE and transferred to nitrocellulose membranes. Membranes were probed using the indicated antibodies. *LIF*, leukemia inhibitory factor.

were probed using the indicated antibodies followed by an IgG-horseradish peroxidase-conjugated secondary antibody (Amersham Biosciences) and visualized with the ECL detection system (Amersham Biosciences). Anti-phospho-ERK1/2 antibodies were purchased from Cell Signaling (Beverly, MA). Anti-phospho-Stat1 and -Stat5 antibodies were obtained from New England Biolabs (Beverly, MA), and anti-Stat1, -Stat3, and -C/EBPα antibodies were purchased from Santa Cruz Biotechnology. Membranes were probed using and visualizes with the ECL detection system (Amersham Biosciences).

Proliferation Assay—32D cl3 and 32Dcl3/DNStat3 cells maintained in IL-3 were washed twice with PBS and starved of cytokine for 8 h and then stimulated with 10 ng/ml G-CSF. The number of viable cells was determined by trypan blue dye exclusion using a hemocytometer. [^{3}H[Thymidine incorporation assays were also performed. Briefly, cells (1×10^5) in 100 μl of medium stimulated with murine IL-3 (1.0 ng/ml) or recombinant human G-CSF (10 ng/ml) were cultured for 48 h. During the final 4 h, [^{3}H]thymidine (1μCi/well) was added. Cells were then harvested by filtration, and radioactivity was counted by scintillation spectrophotometer.

RESULTS

G-CSF-induced Intracellular Signal Response in 32Dcl3/DNStat3 Cells—32Dcl3 cells differentiate into neutrophils following treatment with G-CSF, but 32Dcl3 cells expressing a

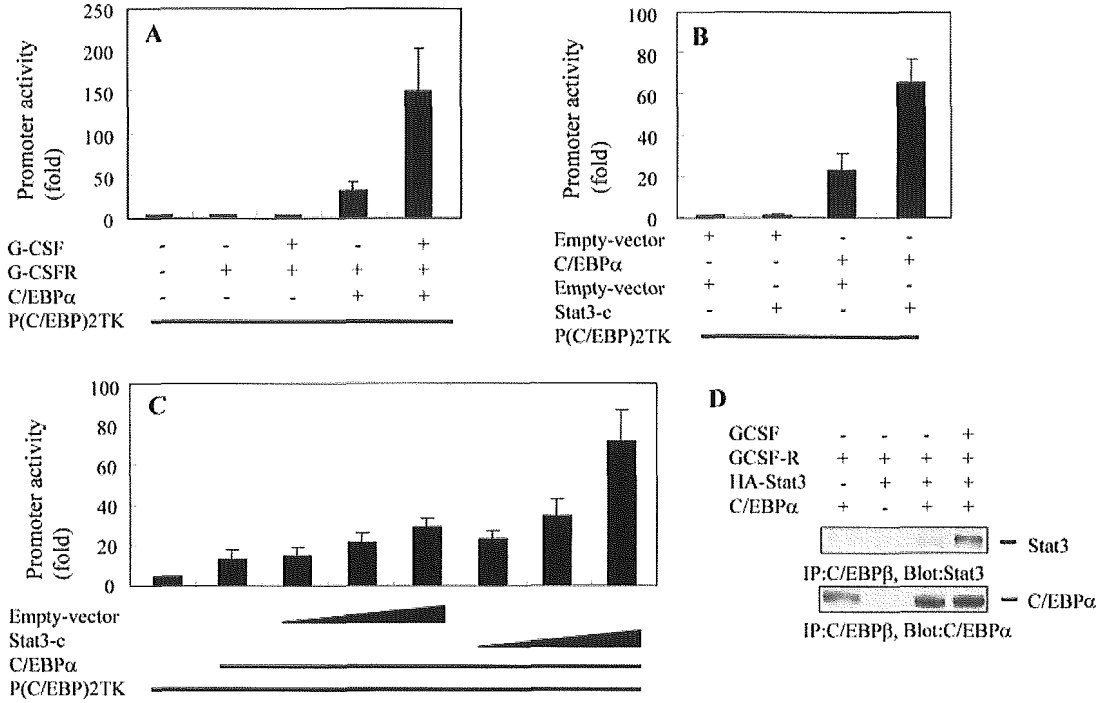

FIG. 4. **Activated Stat3 makes complex with C/EBPα, leading to the enhancement of C/EBPα-induced transcription.** *A*, transient transfection in 293T cells with a reporter construct of a minimal TK promoter with CEBP-binding sites (*p(C/EBP)2TK*), C/EBPα, and G-CSF receptor (*G-CSFR*). Twelve hours after transfection, cells were stimulated with 10 ng/ml G-CSF. Promoter activity was measured as luciferase activity 36 h after transfection. The *vertical axis number* is the fold induction when compared with control. *B* and *C*, transient transfection in 293T cells with a reporter construct of a minimal TK promoter with CEBP-binding sites (*p(C/EBP)2TK*), C/EBPα, Stat3c, and control vectors. Promoter activity was measured as luciferase activity 24 h after transfection. The *vertical axis number* is the fold induction when compared with control. *D*, transient transfection in 293T cells with a construct of G-CSF receptor, HA-Stat3, and C/EBPα and control vectors. After 24 h, cells were lysed and immunoprecipitated (*IP*) with anti C/EBPβ. Cells were stimulated with G-CSF during the final 9 h in the culture. The immunoprecipitates were resolved by 10% SDS-PAGE and transferred to a nitrocellulose membrane. Stat3 was detected by immunoblotting.

dominant-negative Stat3 (32Dcl3/DNStat3) proliferate following G-CSF treatment. These cells maintain immature morphologic characteristics without evidence of differentiation (11). First, we examined the effect of dominant-negative Stat3, carboxyl-truncated Stat3 that lacked 55 amino acids including the transactivation domain. We transfected reporter construct of STATt3-LUC, in which the α2-macroglobulin promoter (16) drives expression of the luciferase (LUC) reporter gene and G-CSF receptor, together with empty vector (pcDNA3) or DNStat3 to 293T cells. After 12 h of transfection, cells were stimulated with 10 ng/ml G-CSF. Cells were cultured for more 24 h, and luciferase assay was performed. As shown in Fig. 1*A*, G-CSF induced the transcriptional activity of Stat3 by 150-fold, and DNStat3 inhibited this G-CSF-induced Stat3 activation in a dose-dependent manner.

G-CSF mainly induces the phosphorylation of Stat3, but it also phosphorylates Stat1 and Stat5 in some cells among the Stats family (8) and induces the activation of MAP kinases. In both 32Dcl3 cells and 32Dcl3/DNStat3 cells, neither Stat1 nor Stat5 was phosphorylated in response to G-CSF (data not shown). As for the MAP kinase activation, the degree of the phosphorylation of ERK1/2 by G-CSF stimulation in 32Dcl3/DNStat3 cells was stronger than that in 32Dcl3 cells (Fig. 1*B*).

Identification of Genes Regulated by Stat3 in the G-CSF Signaling Pathway by Oligonucleotide Array Analysis—To identify Stat3-regulated genes involved in granulocytic differentiation, we compared gene expression change in both cell lines using microarray analysis. 32D cl3 and 32Dcl3/DNStat3 cells maintained in IL-3 were washed twice with PBS and starved in RPMI 1640 containing 10% fetal bovine serum lacking cytokine for 8 h and then stimulated with 10 ng/ml G-CSF. Total RNA was isolated from 32Dcl3 cells and 32Dcl3/DNStat3 cells treated with G-CSF after 0 and 2 h, transcribed to biotin-labeled cRNA, and hybridized to GeneChip MGU74Av2 arrays to compare the expression profile of ~12,000 murine genes. The fold induction in the expression level of each gene was calculated as the ratio of GAPDH-normalized fluorescence intensity value of G-CSF-stimulated cells when compared with those before G-CSF stimulation. As shown in Table I, we could identify a set of candidate genes for Stat3 targets, expression of which was up-regulated in 32D cl3 cells but down-regulated or unchanged in 32Dcl3/DNStat3 cells. Such Stat3-dependent expression profiles were confirmed in triplicate experiments.

C/EBPα Is a Target Gene for Stat3 in G-CSF Signaling Pathway—Among the identified genes, it was decided to focus further efforts on *C/EBPα*. C/EBPα has been shown to be critical for early granulocytic differentiation (17–19), and the factors regulating its activity are unclear. The expression of C/EBPα was examined by real-time quantitative reverse transcription-PCR. C/EBPα mRNA levels are rapidly up-regulated in 32Dcl3 cells, being elevated 2.39-fold after 6 h and 4.20-fold after 48 h (Fig. 2*A*). In contrast to 32Dcl3 cells, the C/EBPα mRNA levels were not changed in 32Dcl3/DNStat3 cells after G-CSF stimulation (Fig. 2*A*). A similar expression pattern was seen in separate experiments with independently designed primers and probes (data not shown). Levels of C/EBPα mRNA were unaffected by cycloheximide treatment (Fig. 2*B*). The expression level of the sum of Stat3 plus dominant-negative Stat3 in 32Dcl3/DNStat3 cells is a little larger than that of Stat3 in 32Dcl3 cells (Fig. 2*C*).

Activated Stat3 Binds to C/EBPα and Enhances the Transcription Activity of C/EBPα—We next examined the effect of

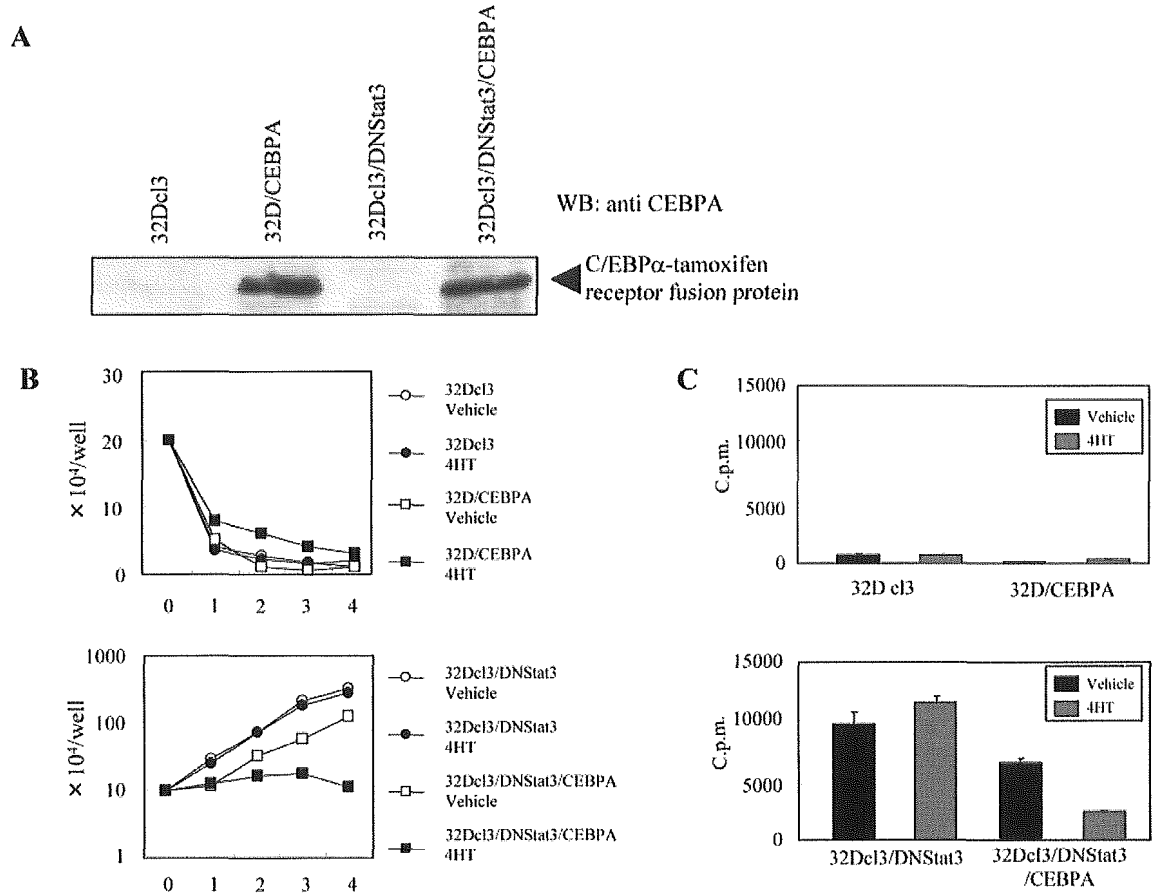

FIG. 5. **Proliferation of 32Dcl3 and 32Dcl3/DNStat3 by restoration of C/EBPα.** *A*, the expression vector pMY-IRES-GFP/C/EBPα-ER was transfected into 32Dcl3 and 32Dcl3/DNStat3 cells. The expression of C/EBPα-ER was examined by Western blotting (*WB*) using anti-C/EBPα polyclonal antiserum. *Lane 1*, 32Dcl3; *lane 2*, 32D/CEBPA; *lane 3*, 32Dcl3/DNStat3; *lane 4*, 32Dcl3/DNStat3/CEBPA. *B*, growth curve of 32Dcl3, 32Dcl3/CEBPA cells (*upper panel*), and 32Dcl3/DNStat3, 32Dcl3/DNStat3/CEBPA cells (*lower panel*). Cells maintained in IL-3 were washed twice with PBS and starved of cytokines for 8 h and stimulated with 10 ng/ml G-CSF plus 0.5 μM 4-HT or vehicle. Viable cells were counted daily by trypan blue dye exclusion method at the indicated times. The *numbers* given on the *vertical axis* represent the mean cell counts ($\times 10^4$/well) of triplicate wells. Standard deviations (S.D.) were less than 15% of each mean. Three independent experiments were performed, and similar results were obtained. Data shown are representative of these results. *C*, ^{3}H incorporation assays in 32Dcl3, 32Dcl3/CEBPA (*upper panel*) and 32Dcl3/DNStat3 and 32Dcl3/DNStat3/CEBPA cells (*lower panel*). Cells maintained in IL-3 were washed twice with PBS and starved of cytokines for 8 h and stimulated with 10 ng/ml G-CSF plus 0.5 μM 4-HT or vehicle for 48 h. During the final 4 h, 1 μCi of [^{3}H]thymidine was added, cells were harvested by filtration, and radioactivity was counted by scintillation spectrophotometer. Results are expressed as mean cpm of triplicate wells ± S.D. Three independent experiments were performed, and similar results were obtained. Data shown are representative of these results.

Stat3 abrogation on the balance of intracellular signals in other cytokine pathways. Although Stat1 was not phosphorylated by leukemia inhibitory factor stimulation in neither 32Dcl3 cells nor 32Dcl3/DNStat3 cells, its activation in response to IFN-γ occurred at the same degree in both 32cl3 cells and 32Dcl3/DNStat3 cells (Fig. 3*A*). As for the Stat5 activation, the phosphorylation of Stat5 by IL-3 stimulation in 32Dcl3 cells was stronger than that in 32Dcl3/DNStat3 cells (Fig. 3*B*). These data indicated that there was the possibility that abrogation of Stat3 signaling can alter the balance of intracellular signals in other cytokine signaling pathways. The transcription of C/EBPα is regulated by C/EBPα itself (20, 21). Then we examined whether activated Stat3 in G-CSF signaling enhance C/EBPα activity or not.

We transfected a reporter construct of a minimal TK promoter with CEBP-binding sites (p(C/EBP)2TK), C/EBPα, and G-CSF receptor to 293T cells. After 12 h of transfection, cells were stimulated with 10 ng/ml G-CSF. Cells were cultured for more 24 h, and a luciferase assay was performed. C/EBPα up-regulated the C/EBPα-dependent gene expression, and the G-CSF stimulation enhanced this C/EBPα-dependent gene expression (Fig. 4*A*). Next we examined the effect of constitutive active Stat3 (Stat3C) on the augmentation of C/EBPα transcriptional activity instead of the G-CSF stimulation. We transfected reporter construct p(C/EBP)2TK, C/EBPα, and Stat3C to 293T cells. After 24 h of transfection, luciferase assay was performed. Stat3C augmented the C/EBPα-dependent gene expression, although Stat3C alone had no influence on the luciferase activity (Fig. 4, *B* and *C*).

As p(C/EBP)2TK contains only a C/EBPα-binding site and does not contain a Stat3-binding sequence, the possibility that Stat3C makes a complex with C/EBPα and augments the function of C/EBPα is raised. Then we transfected C/EBPα, Stat3, and G-CSF receptor to 293T cells and stimulated cells with G-CSF for 6 h. There is no detectable level of endogenous C/EBPα or C/EBPβ protein in 293T cells. Cells were lysed and immunoprecipitated with C/EBPβ antibody (this antibody cross-reacts with C/EBPα). As shown in Fig. 4*D*, immunoprecipitants with anti-C/EBPβ contain Stat3. In addition, the complex formation between C/EBPα and Stat3 is augmented by G-CSF stimulation, indicating that activated Stat3 makes the complex with C/EBPα.

C/EBPα Restores G-CSF-induced Granulocytic Differentiation in 32Dcl3/DNStat3 Cells—To analyze the role of Stat3-

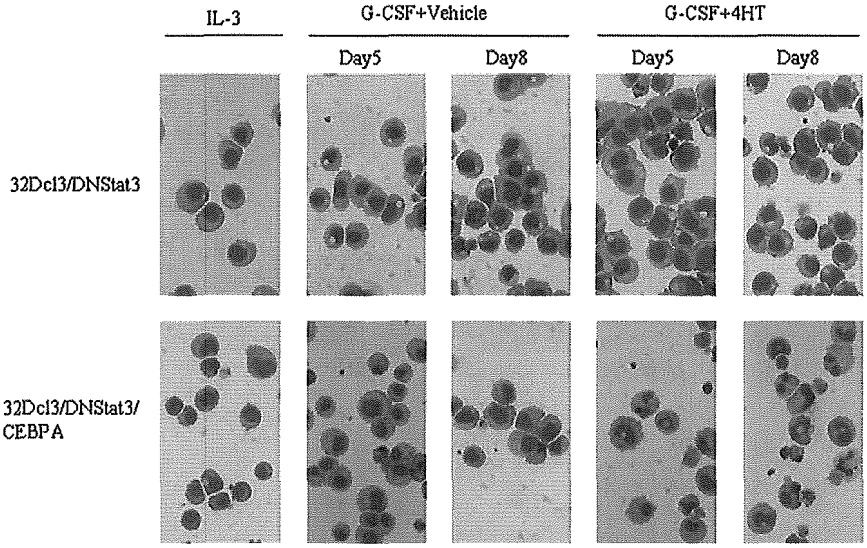

FIG. 6. **Morphologic features of 32Dcl3/DNStat3 and 32Dcl3/DNStat3/CEBPA cells.** Granulocytic differentiation of 32Dcl3/DNStat3 cells after induction of C/EBPα is shown. Cells were maintained in IL-3 and washed twice with PBS and then starved of cytokines for 8 h and stimulated with 10 ng/ml G-CSF plus 0.5 μM 4-HT or vehicle for 5 or 8 days. The cells were cytospun and stained with May-Grunwald and Giemsa stain (original magnification, ×400).

TABLE II
Differential count of 32Dcl3/DNStat3 and 32Dcl3/DNStat3/CEBPA cells

32Dcl3/DNStat3 and32Dcl3/DNStat3/CEBPA cells were maintained in IL-3 and starved of cytokines for 8 h and stimulated with 10 ng/ml G-CSF plus 0.5 μM 4-HT or vehicle for 5 days. Differential count was performed by May-Grunwald and Giemsa stain. Values are the mean ± S.D. percent of cells from three independent experiments. Myelocyte includes promyelocytes, myelocytes, and metamyelocytes. Band(seg) includes band and segmented neutrophils.

Cells	G-CSF+Vehicle	G-CSF+4HT
32Dcl3/DNStat3		
Myeloblasts	98.0 ± 0	99.3 ± 0.47
Myelocytes	1.3 ± 0.94	0.67 ± 0.47
Band(seg)	0.67 ± 0.94	0 ± 0
32Dcl3/DNStat3/CEBPA		
Myeloblasts	90.7 ± 3.3	3.0 ± 2.8
Myelocytes	5.0 ± 0.82	54.3 ± 2.4
Band(seg)	4.3 ± 2.6	42.7 ± 0.47

regulated C/EBPα function in the G-CSF signaling pathway, we transfected a C/EBPα-tamoxifen receptor fusion protein (C/EBPα-ER) into 32Dcl3 and 32Dcl3/DNStat3 cells (32Dcl3/CEBPA cells, 32Dcl3/DNStat3/CEBPA cells, respectively). The expression of C/EBPα-ER in these cells was verified by Western blotting (Fig. 5*A*). C/EBPα-ER localizes to the cytoplasm and is in an inactive form in the absence of tamoxifen. Upon treatment with tamoxifen, it translocates from cytoplasm to nucleus and becomes active. 32Dcl3, 32Dcl3/CEBPA, 32Dcl3/DNStat3, and 32Dcl3/DNStat3/CEBPA cells were cultured with G-CSF in the presence or absence of tamoxifen, and cell proliferation was examined by both counting viable cells and [^{3}H]thymidine incorporation. 32Dcl3/DNStat3 proliferated in response to G-CSF, and proliferation was not affected by the presence of tamoxifen. Conversely, G-CSF-induced proliferation of 32Dcl3/DNStat3/CEBPA cells in the presence of tamoxifen was dramatically reduced (Fig. 5, *B* and *C*).

32Dcl3/DNStat3 cells maintain morphologically immature characteristics and proliferate without granulocytic differentiation after G-CSF stimulation. We examined the morphological changes in 32Dcl3 and 32Dcl3/DNStat3 cells induced by G-CSF after translocation of C/EBPα from the cytoplasm to the nucleus. When tamoxifen was added to medium containing G-CSF, 32Dcl3/DNStat3/CEBPA cells rapidly began to differentiate into granulocytes, and 5 days later, about 40% of the cells were morphologically similar to mature neutrophils. In contrast, 32Dcl3/DNStat3/CEBPA cells cultured in G-CSF-containing medium without tamoxifen appeared immature with blast-like morphologic features (Fig. 6, Table II). To quantitatively analyze the difference in granulocyte maturation in 32Dcl3/DNStat3/CEBPA cells stimulated by G-CSF in the presence of tamoxifen, the mature granulocyte marker Gr-1 was monitored by FACS analysis. 32Dcl3 cells differentiate into Gr-1-positive neutrophils in response to G-CSF (Fig. 7*A*). As shown in Fig. 7*D*, Gr-1-positive cells were increased by the addition of tamoxifen in 32Dcl3/DNStat3/CEBPA cells treated with G-CSF, although low levels were detected in the absence of tamoxifen.

C/EBPα Up-regulates Genes That Are Related to Granulocytic Differentiation—In a conditional expression system, induction of C/EBPα leads to expression of granulocyte-specific genes, such as neutrophil primary granule genes (lysozyme M, *NGAL*) and the G-CSF receptor gene (17). In 32Dcl3/DNStat3 cells, the expression of these genes following G-CSF stimulation was inhibited (Fig. 8, *A*, *C*, and *E*). Interestingly, only *NGAL* was up-regulated by G-CSF in 32Dcl3/DNStat3/CEBPA cells following the restoration of C/EBPα (Fig. 8*B*). Conversely, the expression of lysozyme M and the G-CSF receptor were not changed by the restoration of C/EBPα (Fig. 8, *D* and *F*). These data suggest that regulatory factors in addition to C/EBPα may be involved in the induction of expression of granulocyte-specific genes by G-CSF.

DISCUSSION

G-CSF plays a pivotal role in granulopoiesis and granulocytic differentiation. The binding of G-CSF to its receptor leads to the activation of the Jak-Stat pathway, phosphatidylinositol-3 kinase pathway, and Ras-MAP kinase cascade (22). In the Jak-Stat pathway, G-CSF activates Jak1, Jak2, and Tyk2 followed by the activation of Stat1, Stat3, and Stat5 (7, 8).

Dominant-negative Stat3 inhibits G-CSF-induced transcriptional activity of Stat3 (Fig. 1*A*), as does G-CSF-induced granulocytic differentiation *in vitro* (11). Also, more transgenic mice with a targeted mutation of their G-CSF receptor that abolishes G-CSF-dependent Stat3 activation show severe neutropenia with an accumulation of immature myeloid precursors in their bone marrows (12). Consequently, Stat3 is thought to play an essential role in G-CSF-induced granulocytic differentiation.

32Dcl3 cells differentiate into neutrophils after treatment with G-CSF, and 32Dcl3/DNStat3 cells (32Dcl3 cells expressing dominant-negative Stat3) proliferate in G-CSF without differentiation. The degree of the phosphorylation of ERK1/2 by

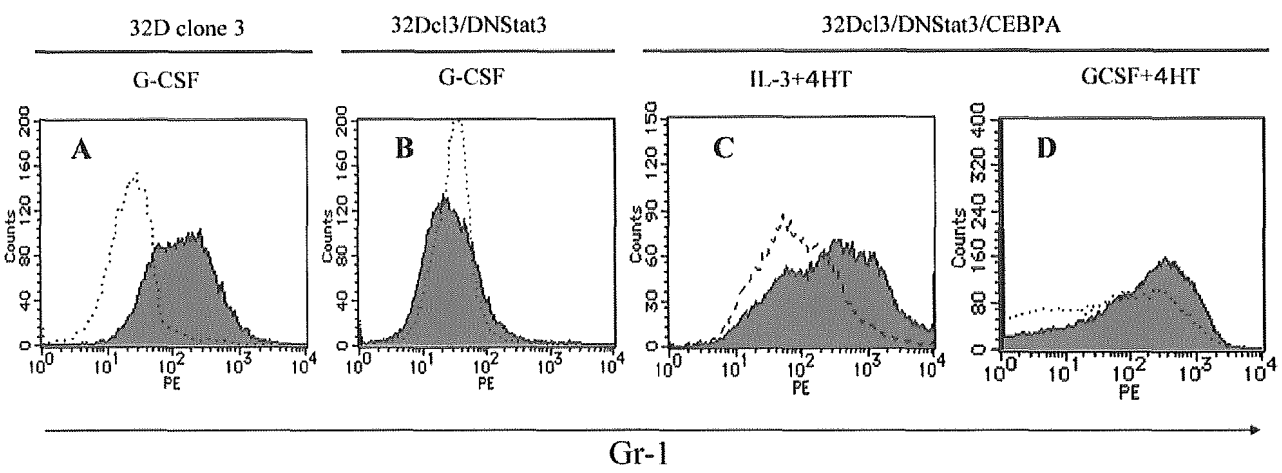

FIG. 7. **The expression of Gr-1 on 32Dcl3, 32Dcl3/DNStat3, and 32Dcl3/DNStat3/CEBPA cells.** 32Dcl3 (*A*) and 32Dcl3/DNStat3 cells (*B*) maintained in IL-3 (*broken line*) were starved of cytokines for 8 h and stimulated with 10 ng/ml G-CSF for 5 days (*solid line*). 32Dcl3/DNStat3/CEBPA (*C*) cells maintained in IL-3 were starved of cytokine for 8 h and stimulated with 1.0 ng/ml IL-3 (*C*) or 10 ng/ml G-CSF (*D*) plus 0.5 μM 4-HT (*solid line*) or vehicle (*broken line*) for 5 days.

G-CSF stimulation in 32Dcl3/DNStat3 cells was stronger than that in 32Dcl3 cells (Fig. 1*B*). We reported that Stat3 null bone marrow cells displayed a significant activation of ERK1/2 after G-CSF stimulation than wild-type bone marrow cells did using Stat3 conditional deficient mice (23). Then the augmented phosphorylation of ERK1/2 in response to G-CSF in 32Dcl3/DNStat3 cells might be caused by the functional abrogation of Stat3 in 32Dcl3/DNStat3 cells.

We compared gene profiles between two cell lines, 32Dcl3 and 32Dcl3/DNStat3 cells, to identify target genes of Stat3 in G-CSF signaling. We found that C/EBPα mRNA levels are rapidly up-regulated in 32Dcl3 cells following G-CSF treatment; these levels are increased 2.39-fold after 6 h and 4.20-fold after 48 h of treatment. In contrast to 32Dcl3 cells, C/EBPα mRNA levels are not changed in 32Dcl3/DNStat3 cells after G-CSF stimulation (Fig. 2*A*). The observation that cycloheximide does not inhibit G-CSF-induced increases in C/EBPα transcript levels (Fig. 2*B*) suggests that C/EBPα is induced by G-CSF directly downstream of Stat3. Dahl *et al.* (24) also reported that G-CSF induced the expression of C/EBPα in IL-3-dependent progenitors. *SOCS3* is one of the major target genes of Stat3. We previously reported that the expression level of SOCS3 protein in Stat3-deficient bone marrow cells is a trace, and it is not augmented by G-CSF stimulation (23). Contrary to this suppression of SOCS3 in Stat3-deficient cells, the induction of SOCS3 by G-CSF is not abolished in 32Dcl3/DNStat3 cells (data not shown).

The phosphorylation of ERK1/2 by G-CSF is stronger and the phosphorylation of Stat5 by IL-3 is weaker in 32Dcl3/DNStat3 cells when compared with those in 32D/Cl3 cells, although Stat1 phosphorylation by IFN-γ was not changed between these two cells (Figs. 1*B* and 3). Then there is the possibility that the transfection of dominant-negative Stat3 affects other signaling pathways in 32Dcl3/DNStat3 cells, resulting in the change of C/EBPα regulation. To clarify whether Stat3 directly up-regulates C/EBPα in the G-CSF signaling pathway in 32Dcl3 cells or not, we examined the effect of Stat3C on the transcription of C/EBPα. C/EBPα up-regulated the C/EBPα-dependent gene expression, and the G-CSF stimulation enhanced this C/EBPα-dependent gene expression (Fig. 4*A*). Strikingly, Stat3C augmented the C/EBPα-dependent gene expression as G-CSF stimulation did (Fig. 4, *B* and *C*). This means that G-CSF-induced up-regulation of C/EBPα-dependent gene expression is, at least partly, due to the activation of Stat3.

Two possibilities arise for the mechanism of the induction of C/EBPα transcription by activated Stat3 in the G-CSF signaling pathway. One is that activated Stat3 binds to the promoter region of *C/EBPα* and induces the transcription of C/EBPα. Analysis of the reported murine *C/EBPα* promoter sequence (20) identified no Stat-responsive elements (TTN5AA) (25, 26), but we found six Stat-responsive elements between 6 and 4 kb upstream of the *C/EBPα* transcription initiation site. Activated Stat3 might bind these Stat-responsive elements between 6 and 4 kb upstream of the C/EBPα transcription initiation site. The other possibility is that activated Stat3 might form the complex with C/EBPα and augment the transcriptional activity of C/EBPα because C/EBPα itself is the only protein reported to activate the murine *C/EBPα* promoter (20, 21). When a minimal TK promoter with CEBP-binding sites (p(C/EBP)2TK) together with C/EBPα was transfected to 293T cells, C/EBPα up-regulated C/EBPα-dependent gene expression. Activated Stat3 (Stat3C) enhanced this C/EBPα-dependent gene expression in collaboration with C/EBPα, although only Stat3C has no transcriptional activity on p(C/EBP)2TK (Fig. 4, *B* and *C*). In addition, the stimulation of G-CSF allows Stat3 to make the complex with C/EBPα (Fig. 4*D*). Then activated Stat3 by G-CSF makes the complex with C/EBPα and augments the transcriptional activity of C/EBPα. This is one of the reasons why induction of C/EBPα transcript through Stat3 activation by G-CSF occurred in 32Dcl3 cells. Several reports have described factors that repress *C/EBPα* promoter activity, such as SP1 (27), AP2A (28), or MYC (29). We show here for the first time that Stat3 augments the *C/EBPα* promoter activity.

Intracellular transcript levels of several genes were changed following G-CSF treatment downstream of Stat3 activation (Table I). To better identify the role of C/EBPα in Stat3-mediated signaling in G-CSF-induced granulocyte differentiation, C/EBPα-ER (C/EBPα-tamoxifen receptor fusion protein) was stably expressed in 32Dcl3 and 32Dcl3/DNStat3 cells. C/EBPα-ER translocates from the cytoplasm to the nucleus and becomes activated upon treatment with tamoxifen. Strikingly, transfection of C/EBPα-ER into 32Dcl3/DNStat3 cells abolished proliferation and induced myeloid differentiation by G-CSF without Stat3 activation (Figs. 5, *B* and *C*, and 6). These data indicate that C/EBPα activation induced by G-CSF through Stat3 plays an essential role in stopping the cell proliferation and inducing the differentiation to the myeloid lineage.

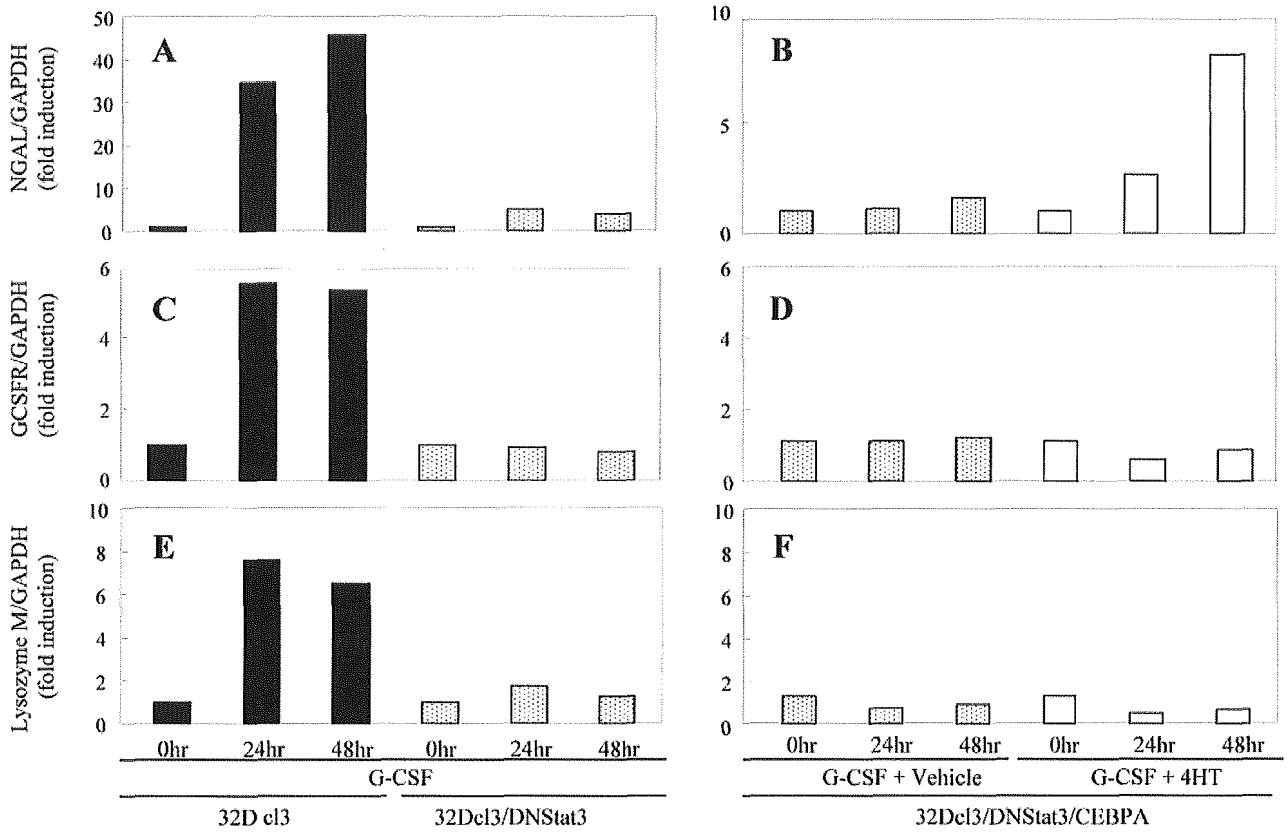

FIG. 8. **Granulocyte-specific gene expressions after C/EBPα induction.** The time course of NGAL (*A* and *B*), G-CSF receptor (*G-CSFR*) (*C* and *D*), and lysozyme M (*E* and *F*) mRNA expression following G-CSF stimulation in 32Dcl3 and 32Dcl3/DNStat3 cells (*A*, *C*, and *E*) or by G-CSF stimulation with 4-HT or vehicle in 32Dcl3/DNStat3/CEBPA cells (*B*, *D*, and *F*) is shown. Cells maintained in IL-3 were starved of cytokines for 8 h and stimulated with G-CSF, G-CSF, plus 4-HT and G-CSF plus vehicle. Total RNA was isolated at the indicated times after the stimulation and transcribed to cDNA, which was subjected to real-time PCR. The *numbers* given on the *vertical axis* represent the fold induction of ratios of average GAPDH-normalized expression values when compared with those before stimulation. Three independent experiments were performed, and similar results were obtained and shown data are the representative of them.

The CEBP family of transcription factor is expressed in multiple cell types, including hepatocytes, adipocytes, keratinocytes, enterocytes, and cells of the lung (30, 31). C/EBPα transactivates the promoters of hepatocyte- and adipocyte-specific genes, which are important for energy homeostasis (32, 33), and *C/EBPα*-deficient mice lack hepatic glycogen stores and die from hypoglycemia within 8 h of birth (34). In the hematopoietic system, C/EBPα is exclusively expressed in myelomonocytic cells (35, 36). C/EBPα expression is prominent in mature myeloid cells, and previous investigations found that C/EBPα is critical for early granulocytic differentiation. Mice with a targeted disruption of the *C/EBPα* gene demonstrate an early block in granulocytic differentiation, but they develop normal monocytes (19). Conditional expression of C/EBPα is sufficient to induce granulocytic differentiation (17). In contrast to the essential role of C/EBPα in granulocytic differentiation, the role of Stat in granulopoiesis is controversial. Stat3 is the principle Stat protein activated by G-CSF, with Stat5 and Stat1 also activated to a lesser degree (8, 10). In mice lacking *Stat5a* and *Stat5b*, the number of colonies produced in response to G-CSF was reduced 2-fold despite normal circulating numbers of neutrophils (9). Myeloid cell lines expressing dominant-negative forms of Stat3 (11, 37, 38) and transgenic mice with a targeted mutation of the G-CSF receptor that abolishes G-CSF-dependent Stat3 activation (12) demonstrate that Stat3-activation is required for G-CSF-dependent granulocytic proliferation and differentiation.

In the present study, we clearly demonstrate that the expression of C/EBPα mRNA is up-regulated through the activation of Stat3 in response to G-CSF, and the Stat3-C/EBPα signaling cascade plays an important role in G-CSF-induced differentiation. Contrary to these data, however, we and others showed that mice conditionally lacking Stat3 in their hematopoietic progenitors developed neutrophilia, and bone marrow cells were hyper-responsive to G-CSF stimulation (23, 39). Additionally, mice with tissue-specific disruption of *Stat3* in bone marrow cells die within 4–6 weeks after birth with Crohn's disease-like pathogenesis (40). These mice exhibit phenotypes with dramatic expansion of myeloid cells, leading to massive infiltration of the intestine with neutrophils, macrophages, and eosinophils. Cells of the myeloid lineage also demonstrate autonomous proliferation. These apparently disparate results may be explained by the need for molecules in addition to Stat3 to regulate C/EBPα expression *in vivo*, the *in vivo* functional redundancy among C/EBPα regulators, or the absence of the abrogation of SOCS3 induction by G-CSF in 32Dcl3/DNStat3 cells. In 32Dcl3 cells, the Stat3-C/EBPα pathway might be favored, and other pathways may contribute little to granulocytic differentiation in response to G-CSF.

Among C/EBP family, C/EBPε is important for late phase of granulocytic differentiation, and its expression is up-regulated by G-CSF independent of Stat3 (11). A previous report showed that C/EBPε is a transcriptional target of C/EBPα in 32Dcl3 cells (41). From these reports and our results, we speculated that a small amount of C/EBPα is enough for the induction of the transcription of C/EBPε by G-CSF or that there are multiple signaling steps except for Stat3-C/EBPα to induce the transcription of C/EBPε by G-CSF.

Induction of C/EBPα led to not only morphologic differentiation but also expression of granulocyte-specific genes (17). In 32Dcl3/DNStat3 cells, the induction of the G-CSF receptor, lysozyme M, and NGAL in response to G-CSF was abrogated (Fig. 8). Restoration of C/EBPα in these cells led to expression of only the *NGAL* gene, and thus, 32Dcl3/DNStat3 cells differentiated by the induction of C/EBPα may not be functional as mature neutrophils. In these cells, therefore, activation of C/EBPα is not sufficient for the induction of lysozyme M or G-CSF receptor genes, and the presence of other molecules appears to be required for their expression.

Acknowledgments—We thank M. Sato, R. Hasegawa, and M. Ito for excellent technical assistance.

REFERENCES

1. Metcalf, D. (1989) *Nature* **339,** 27–30
2. Demetri, G. D., and Griffin, J. D. (1991) *Blood* **78,** 2791–2808
3. Lieschke, G. J., Grail, D., Hodgson, G., Metcalf, D., Stanley, E., Cheers, C., Fowler, K. J., Basu, S., Zhan, Y. F., and Dunn, A. R. (1994) *Blood* **84,** 1737–1746
4. Liu, F., Wu, H. Y., Wesselschmidt, R., Kornaga, T., and Link, D. C. (1996) *Immunity* **5,** 491–501
5. Ihle, J. N., Nosaka, T., Thierfelder, W., Quelle, F. W., and Shimoda, K. (1997) *Stem Cells* **15,** Suppl. 1, 105–111; discussion 112
6. Ihle, J. N. (1995) *Nature* **377,** 591–594
7. Shimoda, K., Iwasaki, H., Okamura, S., Ohno, Y., Kubota, A., Arima, F., Otsuka, T., and Niho, Y. (1994) *Biochem. Biophys. Res. Commun.* **203,** 922–928
8. Shimoda, K., Feng, J., Murakami, H., Nagata, S., Watling, D., Rogers, N. C., Stark, G. R., Kerr, I. M., and Ihle, J. N. (1997) *Blood* **90,** 597–604
9. Teglund, S., McKay, C., Schuetz, E., van Deursen, J. M., Stravopodis, D., Wang, D., Brown, M., Bodner, S., Grosveld, G., and Ihle, J. N. (1998) *Cell* **93,** 841–850
10. Tian, S. S., Lamb, P., Seidel, H. M., Stein, R. B., and Rosen, J. (1994) *Blood* **84,** 1760–1764
11. Nakajima, H., and Ihle, J. N. (2001) *Blood* **98,** 897–905
12. McLemore, M. L., Grewal, S., Liu, F., Archambault, A., Poursine-Laurent, J., Haug, J., and Link, D. C. (2001) *Immunity* **14,** 193–204
13. Fukunaga, R., Ishizaka-Ikeda, E., Seto, Y., and Nagata, S. (1990) *Cell* **61,** 341–350
14. Reddy, V. A., Iwama, A., Iotzova, G., Schulz, M., Elsasser, A., Vangala, R. K., Tenen, D. G., Hiddemann, W., and Behre, G. (2002) *Blood* **100,** 483–490
15. Bromberg, J. F., Wrzeszczynska, M. H., Devgan, G., Zhao, Y., Pestell, R. G., Albanese, C., and Darnell, J. E., Jr. (1999) *Cell* **98,** 295–303
16. Aoki, N., and Matsuda, T. (2002) *Mol. Endocrinol.* **16,** 58–69
17. Radomska, H. S., Huettner, C. S., Zhang, P., Cheng, T., Scadden, D. T., and Tenen, D. G. (1998) *Mol. Cell. Biol.* **18,** 4301–4314
18. Wang, X., Scott, E., Sawyers, C. L., and Friedman, A. D. (1999) *Blood* **94,** 560–571
19. Zhang, D. E., Zhang, P., Wang, N. D., Hetherington, C. J., Darlington, G. J., and Tenen, D. G. (1997) *Proc. Natl. Acad. Sci. U. S. A.* **94,** 569–574
20. Christy, R. J., Kaestner, K. H., Geiman, D. E., and Lane, M. D. (1991) *Proc. Natl. Acad. Sci. U. S. A.* **88,** 2593–2597
21. Legraverend, C., Antonson, P., Flodby, P., and Xanthopoulos, K. G. (1993) *Nucleic Acids Res.* **21,** 1735–1742
22. Ihle, J. N. (1996) *BioEssays* **18,** 95–98
23. Kamezaki, K., Shimoda, K., Numata, A., Haro, T., Kakumitsu, H., Yosie, M., Yamamoto, M., Takeda, K., Matsuda, T., Akira, S., Ogawa, K., and Harada, M. (2005) *Stem Cells* **23,** 252–263
24. Dahl, R., Walsh, J. C., Lancki, D., Laslo, P., Iyer, S. R., Singh, H., and Simon, M. C. (2003) *Nat. Immunol.* **4,** 1029–1036
25. Horvath, C. M., Wen, Z., and Darnell, J. E., Jr. (1995) *Genes Dev.* **9,** 984–994
26. Xu, X., Sun, Y. L., and Hoey, T. (1996) *Science* **273,** 794–797
27. Tang, Q. Q., Jiang, M. S., and Lane, M. D. (1999) *Mol. Cell. Biol.* **19,** 4855–4865
28. Jiang, M. S., Tang, Q. Q., McLenithan, J., Geiman, D., Shillinglaw, W., Henzel, W. J., and Lane, M. D. (1998) *Proc. Natl. Acad. Sci. U. S. A.* **95,** 3467–3471
29. Mink, S., Mutschler, B., Weiskirchen, R., Bister, K., and Klempnauer, K. H. (1996) *Proc. Natl. Acad. Sci. U. S. A.* **93,** 6635–6640
30. Johnson, P. F., Landschulz, W. H., Graves, B. J., and McKnight, S. L. (1987) *Genes Dev.* **1,** 133–146
31. Landschulz, W. H., Johnson, P. F., Adashi, E. Y., Graves, B. J., and McKnight, S. L. (1988) *Genes Dev.* **2,** 786–800
32. Costa, R. H., Grayson, D. R., Xanthopoulos, K. G., and Darnell, J. E., Jr. (1988) *Proc. Natl. Acad. Sci. U. S. A.* **85,** 3840–3844
33. Lin, F. T., and Lane, M. D. (1994) *Proc. Natl. Acad. Sci. U. S. A.* **91,** 8757–8761
34. Wang, N. D., Finegold, M. J., Bradley, A., Ou, C. N., Abdelsayed, S. V., Wilde, M. D., Taylor, L. R., Wilson, D. R., and Darlington, G. J. (1995) *Science* **269,** 1108–1112
35. Scott, L. M., Civin, C. I., Rorth, P., and Friedman, A. D. (1992) *Blood* **80,** 1725–1735
36. Natsuka, S., Akira, S., Nishio, Y., Hashimoto, S., Sugita, T., Isshiki, H., and Kishimoto, T. (1992) *Blood* **79,** 460–466
37. Shimozaki, K., Nakajima, K., Hirano, T., and Nagata, S. (1997) *J. Biol. Chem.* **272,** 25184–25189
38. de Koning, J. P., Soede-Bobok, A. A., Ward, A. C., Schelen, A. M., Antonissen, C., van Leeuwen, D., Lowenberg, B., and Touw, I. P. (2000) *Oncogene* **19,** 3290–3298
39. Lee, C. K., Raz, R., Gimeno, R., Gertner, R., Wistinghausen, B., Takeshita, K., DePinho, R. A., and Levy, D. E. (2002) *Immunity* **17,** 63–72
40. Welte, T., Zhang, S. S., Wang, T., Zhang, Z., Hesslein, D. G., Yin, Z., Kano, A., Iwamoto, Y., Li, E., Craft, J. E., Bothwell, A. L., Fikrig, E., Koni, P. A., Flavell, R. A., and Fu, X. Y. (2003) *Proc. Natl. Acad. Sci. U. S. A.* **100,** 1879–1884
41. Wang, Q. F., and Friedman, A. D. (2002) *Blood* **99,** 2776–2785

ELSEVIER

International Journal of Cardiology 102 (2005) 233–238

International Journal of Cardiology

www.elsevier.com/locate/ijcard

Gene expression profiling of human atrial myocardium with atrial fibrillation by DNA microarray analysis

Ruri Ohki[a], Keiji Yamamoto[a,*], Shuichi Ueno[a], Hiroyuki Mano[b], Yoshio Misawa[c] Katsuo Fuse[c], Uichi Ikeda[a], Kazuyuki Shimada[a]

[a]*Division of Cardiovascular Medicine, Jichi Medical School, Minamikawachi-Machi, Tochigi 329-0498, Japan*
[b]*Division of Functional Genomics, Jichi Medical School, Minamikawachi-Machi, Tochigi 329-0498, Japan*
[c]*Division of Cardiovascular Surgery, Jichi Medical School, Minamikawachi-Machi, Tochigi 329-0498, Japan*

Received 16 December 2003; received in revised form 31 March 2004; accepted 5 May 2004
Available online 9 August 2004

Abstract

Background: Atrial fibrillation (AF) is the most frequently encountered arrhythmia in the clinical setting. However, a comprehensive investigation of the molecular mechanism of AF has not been performed. The aim of this study was to clarify transcriptional profiling of genes modulated in the atrium of AF patients using DNA microarray technology.
Methods: We obtained 17 fresh cardiac specimens, right atrial appendages, isolated from 10 patients with normal sinus rhythm and seven chronic AF patients who underwent cardiac surgery. Affymetrix GeneChip (Human Genome U95A) investigating 12,000 human genes was used for each specimen. Quantitative analysis of selected genes was performed by the real-time PCR method.
Results: The left atrial diameter in the AF group was greater than that in the sinus rhythm group. We could identify 33 AF-specific genes that were significantly activated (>1.5-fold), compared with the sinus rhythm group, including an ion channel, an antioxidant, an inflammation, three cell growth/cell cycle, three transcription such as nuclear factor-interleukin 6-beta, several cell signaling and several protein genes, and seven expressed sequence tags (ESTs). In contrast, we found 63 sinus rhythm-specific genes, including several cell signaling/communication such as sarcoplasmic reticulum Ca^{2+}-ATPase 2, several cellular respiration and energy production and two antiproliferative or negative regulator of cell growth genes, and 22 ESTs.
Conclusions: The present study demonstrated that about one hundred genes were modulated in the atria of AF patients. These findings suggest that these genes may play critical roles in the initiation or perpetuation of AF and the pathophysiology of atrial remodeling.

Keywords: Atrial fibrillation; Genes; Microarray; Myocardium

1. Introduction

Atrial fibrillation (AF) is the most common sustained cardiac arrhythmia and the major cardiac cause of stroke [1]. The Framingham Study [2] reported a sixfold increase in the incidence of stroke in patients with AF, compared with age-, sex-, and blood pressure-adjusted control subjects. In addition, the rapid heart rate resulting from AF can bring about a number of adverse outcomes including congestive heart failure and tachycardia-related cardiomyopathy [3,4]. The molecular research of AF has been focused mainly at various ion channels and at proteins involved in calcium homeostasis, because AF modifies the electrical properties of the atrium in a manner that promotes its occurrence and maintenance. This arrhythmogenic electrophysiological remodeling is well established. However, a comprehensive investigation of the molecular mechanism causing AF has not been performed.

With the recent discovery of the complete sequence of the human genome, as well as the genomes of other organisms, new high-throughput approaches to studying these complex pathways have been made possible. By

* Corresponding author. Tel.: +81 285 58 7344; fax: +81 285 44 5317.
E-mail address: kyamamoto@jichi.ac.jp (K. Yamamoto).

0167-5273/$ - see front matter © 2004 Elsevier Ireland Ltd. All rights reserved.
doi:10.1016/j.ijcard.2004.05.026

Table 1
Patient characteristics

Variable	Total (n=17)	AF (n=7)	Sinus rhythm (n=10)
Age (yrs)	59 ± 16	64 ± 9	56 ± 18
Left atrial diameter (mm)	52 ± 15	67 ± 9*	42 ± 7
LV ejection fraction (%)	60 ± 13	62 ± 13	58 ± 14
MR grade	2.2 ± 1.4	2.7 ± 1.0	1.8 ± 1.0
TR grade	2.0 ± 1.4	2.7 ± 1.0	1.5 ± 1.0
Systolic PA pressure (mmHg)	39.9 ± 14.0	45.0 ± 14.0	35.4 ± 14.0
Mean RA pressure (mmHg)	6.5 ± 3.5	8.6 ± 4.0	4.8 ± 1.0
Digitalis (n)	9	7	2
Systolic blood pressure (mmHg)	133 ± 25	134 ± 26	133 ± 25
Diastolic blood pressure (mmHg)	71 ± 16	75 ± 20	69 ± 13
Fasting blood sugar (mg/dl)	101 ± 15	90 ± 7†	107 ± 15
Total cholesterol (mg/dl)	195 ± 44	208 ± 41	189 ± 46
Triglyceride (mg/dl)	123 ± 64	118 ± 54	125 ± 71

Data are mean ±S.D. or n. *P<0.001 and †P<0.02 compared with sinus rhythm patients. AF, atrial fibrillation; LV, left ventricular; MR, mitral valve regurgitation; PA, pulmonary arterial; RA, right atrial; TR, tricuspid valve regurgitation.

using multiple cDNA or oligonucleotide samples placed on a glass slide, investigators can analyze several thousand full-length genes or expressed oligonucleotide sequences at once. In addition to identifying large clusters of genes that respond to a given stimulus, DNA microarray technology may be used to identify some genes that comprise highly specific molecular responses [5,6]. Already, some studies using microarray technology have yielded interesting results regarding the pathogenesis of cardiovascular diseases, such as myocardial infarction [7], cardiac hypertrophy [8], and human heart failure [9]. In the present study, we used DNA microarray technology to investigate the transcriptional profiling of genes modulated in the right atrium of patients with AF compared with sinus rhythm.

2. Methods

2.1. Subjects

This study group consisted of seven patients with AF (mean age 64±9 years) and 10 patients with sinus rhythm (mean age 56±18 years) who underwent cardiac surgery (Table 1). The underlying heart diseases in the patients are shown in Table 2. Hemodynamic studies were performed the morning after an overnight fast. Vasodilators were withheld for at least 24 h before evaluation. Chronic, stable doses of digoxin, and diuretics were continued but were administered on an evening schedule. Right and left heart studies, including measurement of pressure, biplane left ventriculography and coronary angiography, were performed using a percutaneous cathether. Left ventricular ejection fraction was determined by the area-length method [10]. The severity of mitral regurgitation was assessed according to the method of Sellers et al. [11]. Transthoracic echocardiography was performed in all patients using a Hewlett-Packard SONOS 5500 system (Hewlett-Packard, Palo Alto, CA) with a 2.5 MHz transducer. The left atrial diameter was determined by M-mode echocardiography [12]. The severity of tricuspid regurgitation was graded on a four-point scale, based on the distance reached by the abnormal signals from the tricuspid orifice toward the posterior wall in the parasternal four-chamber view [13].

This study was approved by our institutional human investigations committee, and written informed consent was obtained from all patients before participation.

2.2. Atrial myocardium samples

Right atrial appendages were obtained from the patients during cardiac surgery. Pieces of right atrial appendage weighing 200–1400 mg were frozen immediately in liquid nitrogen, and stored at −80 °C.

Table 2
Underlying heart disease

Patients	Age	Sex	Diagnosis
Sinus group			
1	44	M	AR
2	70	F	MR
3	75	M	AP
4	65	M	AS
5	60	M	AS
6	64	F	MR
7	64	F	AR, MR
8	15	M	ASD
9	63	M	AR
10	36	F	ASD
AF group			
1	51	F	MS
2	55	M	MR
3	64	M	MR
4	74	F	ASR, MSR
5	75	M	ASR, MR
6	59	F	MS
7	69	F	MSR

AP, angina pectoris; AR, aortic valve regurgitation; AS, aortic valve stenosis; ASD, atrial septal defect; ASR, aortic valve stenosis and regurgitation; MR, mitral valve regurgitation; MS, mitral valve stenosis; MSR, mitral valve stenosis and regurgitation.

2.3. Transcriptional profiling

A DNA microarray was used for each specimen. Total RNA was extracted using RNAzol B (TEL-TEST, Friendswood, TX), and the purity was checked by spectrophotometry and agarose gel electrophoresis. Total RNA (5 μg) was converted to double-stranded cDNA using an oligo dT primer containing the T7 promoter (Gibco BRL Superscript® Choice System; Life Technologies, Rockville, MD), and the template for an in vitro transcription reaction was used to synthesize biotin-labeled antisense cRNA (BioArray™ High Yield RNA Transcript Labeling Kit; Enzo Diagnostics, Farmingdale, NY). The biotinylated cRNA was fragmented and hybridized for 16 h at 45 °C to GeneChip Test2 arrays (Affymetrix, Santa Clara, CA) to assess sample quality, and then to Human Genome arrays (U95A, Affymetrix). The arrays were washed, and then stained with streptavidin-phycoerythrin. The arrays were scanned with the GeneArray scanner (Agilent Technologies, Palo Alto, CA) and analyzed using the GeneSpring software package (Silicon Genetics, Redwood City, CA). Human Genome U95A was derived from GenBank 113 and dbEST/10-02-99.

Detailed protocols for data analysis of Affymetrix oligonucleotide microarrays and extensive documentation of the sensitivity and quantitative aspects of the method have been described [14–16]. Briefly, each gene is represented by the use of ~20 perfectly matched (PM) and mismatched (MM) control probes. The MM probes act as specificity controls that allow the direct subtraction of both background and cross-hybridization signals. The number of instances in which the PM hybridization signal is larger than the MM signal is computed along with the average of the logarithm of the PM:MM ratio (after background subtraction) for each probe set. These values are used to make a matrix-based decision concerning the presence or absence of an RNA molecule. Positive average signal intensities after background subtraction were observed for over 12,000 genes for all samples. To determine the quantitative RNA abundance, the average of the differences representing PM minus MM for each gene-specific probe family is calculated, after discarding the maximum, the minimum, and any outliers beyond 3 SDs.

2.4. Real-time reverse transcription (RT)-PCR analysis

For reverse transcription (RT), RNA obtained from each specimen was reverse transcribed using T7-dT primer (5′-TCT AGT CGA CGG CCA GTG AAT TGT AAT ACG ACT CAC TAT AGG GCG TTT TTT TTT TTT TTT TTT TTT-3′) and Superscript II reverse transcriptase (Life Technologies). Real-time quantitative PCR was performed in optical tubes in a 96-well microtiter plate (Perkin-Elmer/Applied Biosystems, Foster City, CA) with an ABI PRISM 7700 Sequence Detector Systems (Perkin-Elmer/Applied Biosystems) according to the manufacturer's instructions. By using the SYBR Green PCR Core Reagents Kit (Perkin-Elmer/Applied Biosystems, P/N 4304886), fluorescence signals were generated during each PCR cycle via the 5′-to 3′-endonuclease activity of Taq Gold [17] to provide real-time quantitative PCR information. The oligonucleotide primers used for real-time PCR analysis are shown in Table 3. No template controls as well as the samples were added in a total volume of 50 μl/reaction. Potential PCR product contamination was digested by uracil-*N*-glycosylase, because dTTP is substituted by dUTP [17]. All PCR experiments were performed with the hot start method. In the reaction system, uracil-*N*-glycosylase and Taq Gold (Perkin-Elmer/Applied Biosystems) were applied according to the manufacturer's instructions [17,18]. Denaturing and annealing reactions were performed 40 times at 95 °C for 15 s, and at 60 °C for sarcoplasmic reticulum Ca^{2+}-ATPase 2, 66 °C for nuclear factor-interleukin 6 (NF-IL6)-beta and 62 °C for glyceraldehyde-3 phosphate dehydrogenase (GAPDH) for 1 min, respectively. The increase in the fluorescence signal is proportional to the amount of specific product [14]. The intensity of emission signals in each sample was normalized to that of GAPDH as an internal control.

2.5. Statistical analysis

Raw data from array scans were averaged across all gene probes for each array, and a scaling factor was applied to bring the average intensity for all probes on the array to 2500. This allows any sample to be normalized for comparison with any other comparable sample.

Table 3
Primer design for real-time PCR analysis

Gene		Primer sequence	PCR product size (bp)
NF-IL6-beta	Sense	5′-CACAGACCGTGGTGAGCTTG-3′	257
	Antisense	5′-CACCAACTTCTGCTGCATCTC-3′	
Sarcoplasmic reticulum	Sense	5′-TTTCTGGTACAAACATTGCTGC-3′	140
Ca^{2+}-ATPase 2	Antisense	5′-TAGTTTTTGCTGAAGGGGTGTT-3′	
GAPDH	Sense	5′-CTTTGGTATCGTGGAAGGACTC-3′	140
	Antisense	5′-CAGTAGAGGCAGGGATGATGTT-3′	

GAPDH, glyceraldehyde-3 phosphate dehydrogenase; NF-IL6, nuclear factor-interleukin 6.

Table 4
Analysis of AF-specific genes by DNA microarray

Function	Gene	Fold change	Genbank#
Antioxidants	Glutathione peroxidase	1.8 ± 1.1	X13710
Cell growth	Vascular endothelial growth factor B	1.6 ± 0.7	U43368
Cell signaling	RhoC	1.6 ± 0.5	L25081
Inflammation	Macrophage migration inhibitory factor	1.7 ± 0.6	L19686
Proto-oncogene	A-raf-1 oncogene	1.5 ± 0.5	U01337
Transcription	NF-IL6-beta	2.0 ± 0.7	M83667

Data are mean ±S.D. Fold change was relative to sinus rhythm group. NF-IL6, nuclear factor-interleukin 6.

Data are expressed as the mean ± S.D. Differences were analyzed with the Mann–Whitney *U* test for unpaired observations. A *P*-value of <0.05 was considered significant.

3. Results

3.1. Patient characteristics

As shown in Table 1, the left atrial diameter in the AF group was significantly greater than that in the sinus rhythm group ($P<0.001$). In addition, the levels of fasting blood sugar in the AF group were significantly lower than those in the sinus rhythm group ($P<0.02$). There were no other differences detected between the sinus rhythm group and AF group.

3.2. DNA microarray analysis of AF-specific genes

We identified 33 AF-specific genes that were significantly activated (>1.5-fold, $P<0.05$), compared with those in the sinus rhythm group, including an ion channel, an antioxidant, an inflammation, three cell growth/cell cycle, three transcription, several cell signaling and several protein genes, and seven expressed sequence tags (ESTs). Some of the selected genes are shown in Table 4. All data are available in an online only Data Supplement at http://www.elsevier.com/locate/inca/506041.

3.3. DNA microarray analysis of sinus rhythm-specific genes

In contrast, we found 63 sinus rhythm-specific genes, including several cell signaling/communication genes such as sarcoplasmic reticulum Ca^{2+}-ATPase 2, several cellular respiration and energy production and two antiproliferative or negative regulator of cell growth genes, and 22 ESTs (<0.5-fold, $P<0.05$). Some of the selected genes are shown in Table 5. All data are available in an online only Data Supplement at http://www.elsevier.com/locate/inca/506041.

3.4. Real-time RT-PCR analysis

We focused on two of the genes screened by the oligonucleotide microarray: NF-IL6-beta and sarcoplasmic reticulum Ca^{2+}-ATPase 2. NF-IL6-beta is an important transcriptional activator in the regulation of genes involved in the immune and inflammatory response [19]. AF may persist due to structural changes in the atria that are promoted by inflammation [20]. In addition, cytosolic Ca^{2+} overload may be an important mediator of AF. Abnormalities in the Ca^{2+} regulatory proteins, such as sarcoplasmic reticulum Ca^{2+}-ATPase 2, of the atrial myocardium in chronic AF patients may be involved in the initiation and/or perpetuation of AF. These genes were confirmed by the real-time RT-PCR method. As shown in Fig. 1, NF-IL6-beta mRNA expression in the AF group was significantly higher than that in the sinus rhythm group ($P<0.02$). In contrast, as shown in Fig. 2, sarcoplasmic reticulum Ca^{2+}-ATPase 2 mRNA expression in the AF group was lower compared with that in the sinus rhythm group ($P<0.1$), but not significantly.

4. Discussion

The cellular and molecular basis of AF has been a field of enormous interest over the past few years. However, the

Table 5
Analysis of sinus rhythm-specific genes by DNA microarray

Function	Gene	Fold change	Genbank#
Antioxidants	Peroxiredoxin 3	0.5 ± 0.2	D49396
Cell signaling	Caveolin 2	0.4 ± 0.3	AF035752
Cell signaling	Sarcoplasmic reticulum Ca^{2+}-ATPase 2	0.4 ± 0.3	M23115
Cell signaling	Connexin 43	0.4 ± 0.3	X52947
Proto-oncogene	Ras-associated protein rab1	0.5 ± 0.2	AL050268

Data are mean ±S.D. Fold change was relative to sinus rhythm group.

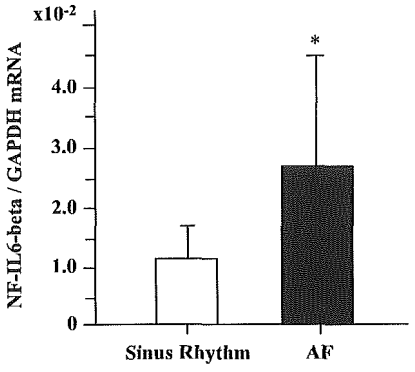

Fig. 1. Nuclear factor-interleukin 6 (NF-IL6)-beta mRNA expression in the right atria of patients with sinus rhythm and atrial fibrillation (AF). Total RNA obtained from the right atria of patients with sinus rhythm (n=10) and AF (n=7) using RNAzol B (TEL-TEST) was analyzed by quantitative real-time reverse transcription-PCR as described in Methods. The amount of mRNA expression for NF-IL6-beta was standardized to that of glyceraldehyde-3 phosphate dehydrogenase (GAPDH) mRNA expression. Data are means±S.D. *P<0.02 compared with sinus rhythm patients.

mechanism of AF in human tissues is extremely complex, because atrial remodeling consists of electrical, contractile, and structural remodeling. In addition, structural remodeling may occur from chronic hemodynamic, metabolic, or inflammatory stressors. Many factors such as ion channels, proteins influencing calcium homeostasis, connexins, autonomic innervation, fibrosis, paracrine factors, and cytokines may be involved in the molecular mechanism of AF. The present study using oligonucleotide microarray analysis demonstrated that about one hundred genes were modulated in the right atrium of patients with AF. These findings suggest that these genes may play critical roles in the initiation or perpetuation of AF and the pathophysiology of atrial remodeling.

In the present study, DNA microarray analysis identified 33 AF-specific genes. Some of these genes encode NF-IL6-beta, macrophage migration inhibitory factor, A-raf-1 oncogene, vascular endothelial growth factor B, RhoC, and glutathione peroxidase. NF-IL6-beta mRNA expression induced in the atria of AF patients was confirmed by the real-time PCR method. NF-IL6-beta and macrophage migration inhibitory factor are involved in inflammation [19,21]. Chung et al. [20] reported that C-reactive protein, a marker of systemic inflammation, is elevated in AF patients compared with sinus rhythm patients. Novel and inflammatory mechanisms may promote the persistence of AF, potentially by inducing structural and/or electrical remodeling of the atria. A-raf-1 protooncogene encodes cytoplasmic protein serine/threonine kinase, which plays an important role in cell growth and development [22]. Vascular endothelial growth factor B with structural similarities to vascular endothelial growth factor and placenta growth factor has a role in angiogenesis and endothelial cell growth [23]. RhoC, small guanosine triphosphatase Rho, which regulates remodeling of the actin cytoskeleton during cell morphogenesis and motility [24], may contribute to the structural remodeling. Baumer et al. [25] demonstrated that the activity, mRNA, and protein levels of glutathione peroxidase, an antioxidative enzyme, decreased in human failing myocardium. However, the present study showed that the glutathione peroxidase mRNA level in AF patients was elevated.

The present study demonstrated that the expression of 63 genes in AF patients was significantly lower compared with sinus rhythm. For example, genes for sarcoplasmic reticulum Ca^{2+}ATPase 2 and connexin 43 in AF patients were downregulated. In the real-time PCR analysis, sarcoplasmic reticulum Ca^{2+}-ATPase 2 mRNA expression in the AF group was lower compared with that in the sinus rhythm group, but not significantly. Ohkusa et al. [26] also reported that sarcoplasmic reticulum Ca^{2+}-ATPase 2 mRNA in both the right and left atrial myocardial tissues from 13 patients with AF were significantly lower than in the right atrium of patients with sinus rhythm. A decrease in sarcoplasmic reticulum Ca^{2+}-ATPase 2 in the atria may sustain abnormal intracellular Ca^{2+} handling and changes in the electrophysiologic properties of atrial tissue, leading to the perpetuation of AF. Connexin 43 is one of the gap junctions that are clusters of closely packed channels. Gap junctions directly connect the cytoplasmic compartments of neighboring cells and allow the passage of ions and small molecules. In the present study, connexin 43 mRNA expression in AF patients was downregulated. It is still controversial whether connexin 43 is upregulated [27], unchanged or downregulated in AF. Thus, changes in the expressions of connexin 43 might affect conduction velocity, contributing to sustained AF.

Previous studies demonstrated that some genes including L-type calcium channel [28], potassium channels [29], and sarcoplasmic reticulum Ca^{2+}-ATPase 2 [26,28] are modulated in AF patients. However, the molecular

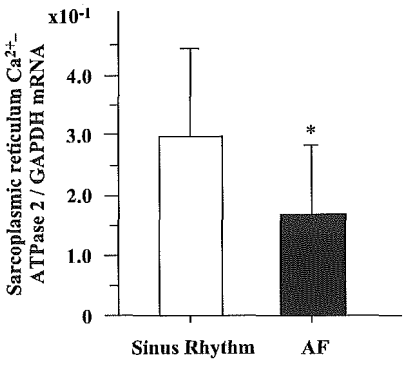

Fig. 2. Sarcoplasmic reticulum Ca^{2+}-ATPase 2 mRNA expression in the right atria of patients with sinus rhythm and atrial fibrillation (AF). Total RNA obtained from the right atria of patients with sinus rhythm (n=10) and AF (n=7) using RNAzol B (TEL-TEST) was analyzed by quantitative real-time reverse transcription-PCR as described in Methods. The amount of mRNA expression for sarcoplasmic reticulum Ca^{2+}-ATPase 2 was standardized to that of glyceraldehyde-3 phosphate dehydrogenase (GAPDH) mRNA expression. Data are means±S.D. *P<0.1 compared with sinus rhythm patients.

mechanism of AF is poorly understood. Although the roles of other genes including ESTs in the heart except for the genes described above still remain unknown, the genes screened in this study may provide insights into the initiation or perpetuation of AF and the pathophysiology of atrial remodeling, because DNA microarray is a highly effective method for screening genes.

Acknowledgements

This study was supported by grants from the Ministry of Education, Science, Sports and Culture of Japan (15590769), Tokyo, Japan, the Mitsui Life Social Welfare Foundation, Tokyo, Japan, the Takeda Science Foundation, Osaka, Japan, the Daiwa Securities Health Foundation, Tokyo, Japan, and the Sankyo Foundation of Life Science, Tokyo, Japan.

References

[1] Cerebral Embolism Task Force. Cardiogenic brain embolism. Arch Neurol 1986;43:71–84.
[2] Wolf PA, Dawber TR, Thomas Jr HE, Kannel WB. Epidemiologic assessment of chronic atrial fibrillation and risk of stroke: the Framingham study. Neurology 1978;28:973–7.
[3] Okishige K, Sasano T, Yano K, Azegami K, Suzuki K, Itoh K. Serious arrhythmias in patients with apical hypertrophic cardiomyopathy. Intern Med 2001;40:396–402.
[4] Redfield MM, Kay GN, Jenkins LS, Mianulli M, Jensen DN, Ellenbogen KA. Tachycardia-related cardiomyopathy: a common cause of ventricular dysfunction in patients with atrial fibrillation referred for atrioventricular ablation. Mayo Clin Proc 2000;75:790–5.
[5] Iyer VR, Eisen MB, Ross DT, et al. The transcriptional program in the response of human fibroblasts to serum. Science 1999;283:83–7.
[6] Feng Y, Yang JH, Huang H, et al. Transcriptional profile of mechanically induced genes in human vascular smooth muscle cells. Circ Res 1999;85:1118–23.
[7] Stanton LW, Garrard LJ, Damm D, et al. Altered patterns of gene expression in response to myocardial infarction. Circ Res 2000;86:939–45.
[8] Friddle CJ, Koga T, Rubin EM, Bristow J. Expression profiling reveals distinct sets of genes altered during induction and regression of cardiac hypertrophy. Proc Natl Acad Sci U S A 2000;97:6745–50.
[9] Yang J, Moravec CS, Sussman MA, et al. Decreased SLIM1 expression and increased gelsolin expression in failing human hearts measured by high-density oligonucleotide arrays. Circulation 2000;102:3046–52.
[10] Greene DG, Carlisle R, Grant C, Bunnell IL. Estimation of left ventricular volume by one-plane cineangiography. Circulation 1967;35:61–9.
[11] Sellers RD, Levy MJ, Amplatz K, Lillehei CW. Left retrograde cardioangiography in acquired cardiac disease: technic, indications and interpretation in 700 cases. Am J Cardiol 1964;14:437–47.
[12] Sahn DJ, DeMaria A, Kisslo J, Weyman A. Recommendations regarding quantitation in M-mode echocardiography: results of a survey of echocardiographic measurements. Circulation 1978;58: 1072–1083.
[13] Miyatake K, Okamoto M, Kinoshita N, et al. Evaluation of tricuspid regurgitation by pulsed Doppler and two-dimensional echocardiography. Circulation 1982;66:777–89.
[14] Lockhart DJ, Dong H, Byrne MC, et al. Expression monitoring by hybridization to high-density oligonucleotide arrays. Nat Biotechnol 1996;14:1675–80.
[15] Lee CK, Klopp RG, Weindruch R, Prolla TA. Gene expression profile of aging and its retardation by caloric restriction. Science 1999; 285:1390–3.
[16] Golub TR, Slonim DK, Tamayo P, et al. Molecular classification of cancer: class discovery and class prediction by gene expression monitoring. Science 1999;286:531–7.
[17] Heid CA, Stevens J, Livak KJ, Williams PM. Real time quantitative PCR. Genome Res 1996;6:986–94.
[18] Kruse N, Pette M, Toyka K, Rieckmann P. Quantification of cytokine mRNA expression by RT PCR in samples of previously frozen blood. J Immunol Methods 1997;210:195–203.
[19] Kinoshita S, Akira S, Kishimoto T. A member of the C/EBP family, NF-IL6 beta, forms a heterodimer and transcriptionally synergizes with NF-IL6. Proc Natl Acad Sci U S A 1992;89:1473–6.
[20] Chung MK, Martin DO, Sprecher D, et al. C-reactive protein elevation in patients with atrial arrhythmias: inflammatory mechanisms and persistence of atrial fibrillation. Circulation 2001;104:2886–91.
[21] Bacher M, Metz CN, Calandra T, et al. An essential regulatory role for macrophage migration inhibitory factor in T-cell activation. Proc Natl Acad Sci U S A 1996;93:7849–54.
[22] Lee JE, Beck TW, Brennscheidt U, DeGennaro LJ, Rapp UR. The complete sequence and promoter activity of the human A-raf-1 gene (ARAF1). Genomics 1994;20:43–55.
[23] Olofsson B, Pajusola K, Kaipainen A, et al. Vascular endothelial growth factor B, a novel growth factor for endothelial cells. Proc Natl Acad Sci U S A 1996;93:2576–81.
[24] Mackawa M, Ishizaki T, Boku S, et al. Signaling from Rho to the actin cytoskeleton through protein kinases ROCK and LIM-kinase. Science 1999;285:895–8.
[25] Baumer AT, Flesch M, Wang X, Shen Q, Feuerstein GZ, Bohm M. Antioxidative enzymes in human hearts with idiopathic dilated cardiomyopathy. J Mol Cell Cardiol 2000;32:121–30.
[26] Ohkusa T, Ueyama T, Yamada J, et al. Alterations in cardiac sarcoplasmic reticulum Ca^{2+} regulatory proteins in the atrial tissue of patients with chronic atrial fibrillation. J Am Coll Cardiol 1999;34:255–63.
[27] van der Velden HM, Ausma J, Rook MB, et al. Gap junctional remodeling in relation to stabilization of atrial fibrillation in the goat. Cardiovasc Res 2000;46:476–86.
[28] Brundel BJ, van Gelder IC, Henning RH, et al. Gene expression of proteins influencing the calcium homeostasis in patients with persistent and paroxysmal atrial fibrillation. Cardiovasc Res 1999;42:443–54.
[29] Brundel BJ, VanGelder IC, Henning RH, et al. Alterations in potassium channel gene expression in atria of patients with persistent and paroxysmal atrial fibrillation: differential regulation of protein and mRNA levels for K+channels. J Am Coll Cardiol 2001;37:926–32.

CMLS, Cell. Mol. Life Sci. 62 (2005) 2140–2146
1420-682X/05/182140-7
DOI 10.1007/s00018-005-5270-5

CMLS Cellular and Molecular Life Sciences

Research Article

Regulation of *Amh* during sex determination in chickens: *Sox* gene expression in male and female gonads

S. Takada[a, b], H. Mano[b] and P. Koopman[a, *]

[a] Institute for Molecular Bioscience, The University of Queensland, Brisbane, Queensland 4072 (Australia), Fax: +61 7 3346 2101, e-mail: p.koopman@imb.uq.edu.au
[b] Division of Functional Genomics, Jichi Medical School, 3311-1 Yakushiji, Minamikawachimachi, Kawachigun, Tochigi 329-0498 (Japan)

Received 18 June 2005; received after revision 22 June 2005; accepted 27 June 2005
Online First 26 August 2005

Abstract. During mammalian sexual development, the SOX9 transcription factor up-regulates expression of the gene encoding anti-Müllerian hormone (AMH), but in chickens, *Sox9* gene expression reportedly occurs after the onset of Amh expression. Here, we examined expression of the related gene *Sox8* in chicken embryonic gonads during the sex-determining period. We found that *cSox8* is expressed at similar levels in both sexes at embryonic day 6 and 7, and only at the anterior tip of the gonad, suggesting that SOX8 is not responsible for the sex-specific increase in *cAmh* gene expression at these stages. We also found that several other chicken *Sox* genes (*cSox3*, *cSox4* and *cSox11*) are expressed in embryonic gonads, but at similar levels in both sexes. Our data suggest that the molecular mechanisms involved in the regulation of *Amh* genes of mouse and chicken are not conserved, despite similar patterns of *Amh* expression in both species.

Key words. Sex determination; Amh; chicken; testis.

Even though molecular mechanisms of patterning and morphogenesis are surprisingly well conserved during metazoan evolution, mechanisms governing sex determination and gonadal development are diverse, even among vertebrates. In mammals, the heterogametic pairing of sex chromosomes (XY) results in male development. The mouse and human sex-determining gene, *Sry/SRY* (sex-determining region on Y chromosome), has been identified [1, 2] and is known to cause the bipotential gonad to differentiate into a testis [3]. However, *Sry* is not a conserved sex-determining gene as it exists only in mammals [4–7]. In contrast to mammals, in birds males are homogametic (ZZ) and females are heterogametic for the sex chromosomes (ZW). Whether avian sex is determined by a master female-determining gene on the W chromosome or by Z chromosome gene dosage is still unclear [8].

There are reports for the mouse that several genes are expressed predominantly in the developing testis but not in the ovary and, therefore, are likely to be important for male sex determination and differentiation. Some of these genes, such as *Amh* (anti-Müllerian hormone) and *Sox9* [9–12] are expressed similarly in mouse and chicken gonads, suggesting that there could be some degree of similarity between the molecular pathways and sexual development in chicken and mouse. However, some differences are evident. For example, *Sf1* (steroidogenic factor 1) and *Gata4* are predominantly expressed in the male gonad in mice [13, 14], while in chicken expression levels of both genes are similar between male and female gonads [12, 15].

* Corresponding author.